PROSPECTS FOR ATOMIC FREQUENCY STANDARDS

by

C. Audoin

Laboratoire de l'Horloge Atomique
Equipe de Recherche du CNRS,
associée à l'Université Paris-Sud
Bât. 221 - Université Paris-Sud
91405 Orsay, France

ABSTRACT

We shall describe the potentialities of different atomic frequency standards which are not yet into field operation, for most of them, but for which preliminary data, obtained in laboratory experiments, give confidence that they may improve greatly the present state of the art.

The review will mainly cover the following devices :
- cesium beam frequency standards with optical pumping and detection
- optically pumped rubidium cells
- magnesium beam
- cold hydrogen masers
- traps with stored and cooled ions.

1. PHYSICAL BACKGROUND

Atomic frequency standards are founded on the space and time invariance of the energy difference between specified levels of atoms, at rest and in a given acceleration field. This statement is to be related to the absence of experimental evidence of a cosmological variation of the fundamental constants, at least at the present level of our measurement ability.

However, there are two fundamental limits to the precision of the measurement of the energy difference $h\nu$ between two atomic levels.

The first one is set by the Heisenberg uncertainty principle, $\Delta\nu \cdot \Delta t = 1$, which means that the linewidth cannot be smaller than the inverse of the observation time, about. This limit may be reached provided that appropriate tricks eliminate as well as possible other sources of line broadening such as the first order Doppler effect and the inhomogeneity of the static magnetic field, for instance.

Assuming that these spurious effects are under sufficiently good control, the Heisenberg principle call for long interaction times such as in the hydrogen maser and in ion traps.

The second fundamental limit is determined by noise processes. In the case where the atomic resonance is monitored by a flux of particles, atoms or photons, shot noise is the annoying effect. The corresponding fractional fluctuations of the particle flux being inversely proportional to the mean flux value, it is desirable to monitor a high particle flux, in atomic beam devices for instance. In the hydrogen maser, where the atomic transition is detected whether as the creation (active operation), or the variation (passive operation), of a coherent electromagnetic field, thermal noise due to the brownian motion of electrons in the cavity wall perturbs the phase and the amplitude of the electromagnetic field. The most obvious solution -at least in principle- consists in the cooling of the cavity.

A more detailed analysis shows that the fractional frequency stability measure, $\sigma_y(\tau)$ [1], is given by :

$$\sigma_y(\tau) \simeq \frac{1}{Q\ S/B(\tau)} \tag{1}$$

where Q is the quality factor of the atomic line and $S/B(\tau)$ the signal to noise ratio of its observation,during the time interval τ. The best frequency stability is then obtained in devices where it is possible to realize both a large quality factor and a large signal to noise ratio. Of course, tradeoffs between the two factors are possible.

A high quality factor requires, among other demands, a sufficiently large transition frequency. At the present time, the largest one which has been used in experimental devices are that of the hyperfine transition of the mass 199 mercury ion, at 40.5 GHz, and that of a fine structure transition of the mass 24 magnesium atom at 601 GHz. At the present time, higher frequencies cannot be produced and/or measured in sufficiently reliable set-ups, so that we shall focus on microwave frequency standards, mainly.

The preceding remarks indicate the directions in which improvements of atomic frequency standards may be expected. They refer, in fact, to means of enhancing the short and medium term frequency stability. However, it is well known that other qualities are necessary to fulfill the present demand. Among them, the long term stability and the reproducibility are of prime importance in a num-

her of applications. Similarly, improved accuracy is desired for the laboratory primary cesium beam frequency standards, which realize the definition of the S.I. time unit. As we will see, the cited directions of work are also beneficial to those very important characteristics. Their improvement motivates, in particular, the present efforts to cool ions and to observe one of a few of them almost at rest and isolated from spurious sources of frequency shifts.

A description of the principles and of the design of most of the existing frequency standards has been given in review articles [2,3] and shall not be repeated here.

2. BASIC PROPERTIES OF THE USEFUL TRANSITIONS

Hyperfine transitions of atoms and ions in the ground state share in common the following properties of interest :

- the life-time of the hyperfine levels is very large, amounting to years, due to the very low probability of spontaneous emission. This is mainly related to the small energy difference $h\nu_0$ between the levels,

- the Stark effect, i.e. the frequency shift due to an electric field E is of second order,

- the Zeeman effect of some of the $\Delta F = 1$, $\Delta m_F = 0$ transitions is also of second order. The sensitivity to the magnetic field of the fine structure transition in ^{24}Mg is very small. It is approximately equal to 10^{-4} times that of cesium [4]. Table 1 gives some pertinent numerical values.

As a result of the small energy difference between the ground state hyperfine levels, they are almost equally populated at thermal equilibrium, such as in an atomic beam source. State selection is then mandatory to observe hyperfine transitions with a sufficient signal to noise ratio. This is accomplished either by magnetic deflection or optical pumping.

In the case of the magnesium fine structure transition, atoms are produced in a metastable state having three sublevels with different lifetimes. The population difference follows from the fastest decay to the ground state of one of them.

3. BEAM FREQUENCY STANDARDS WITH OPTICAL PUMPING AND DETECTION

3.1. Cesium Beam

a) Experimental achievements

In 1950, A. Kastler [5] showed that it shoud be possible to optically enhance the population of certain atomic levels and to optically detect magnetic resonance transitions. He suggested that the strong and inhomogeneous magnetic field regions could be replaced by optical interaction region in the Rabi beam magnetic resonance machine. This possibility was confirmed in a Rb 87 beam using rubidium spectral lamps and a Ramsey-type microwave cavity [6]. However, at that time, the light sources were spectral lamps, and the energy density of the light beam was not large enough to provide efficient optical pumping and detection. More recently, the development of reliable semi-conductor laser light sources in the near infrared, at 0.852 μm, enabled the optical pumping of cesium atoms and the optical detection of the F = 4, m_F = 0 $\longleftrightarrow$ F = 3, m_F = 0 clock transition at 9.192 MHz produced in a Ramsey type microwave cavity [7].

Figure 1 shows the principle of optical pumping and detection. At the left of the figure an energy diagram is shown with two levels in the ground state and one in an excited state. A light beam excites the atoms from level 1 to 3. The population of the excited state decays by spontaneous emission with an equal probability on levels 1 and 2. Assuming that the energy density is large enough it follows that the level 2 is populated at the detriment of level 1, and a population difference is created by optical pumping. This three level configuration is also useful for the detection of a transition between levels 1 and 2. If this transition occurs, the level 2 becomes populated and the light beam may transfer one atom to level 3. Spontaneous emission creates one fluorescence photon which may be detected and used to monitor the 1 $\longleftrightarrow$ 2 transition. In that case, one photon at most is produced per atom. Another optical detection scheme is shown at the right of figure 1. Only two levels are involved. One fluorescence photon is emitted each time one photon of the incident light beam is absorbed by atoms in level 1. The life-time of the excited state being very small, one may then detect several photons per atom if the light beam energy density is sufficiently large. This transition is denoted as a cycling transition. Furthermore, the number of photons is proportional to the time spent by the atoms in the light beam, and, consequently, this method provides a narrowing of the line.

The configurations of figure 1 are included in the level energy diagram of the cesium atom, shown in figure 2, in a simplified form. Taking into account the selection rule ΔF = 0 or $\pm$ 1, one sees that the levels F = 3 and 4 of the ground state plus the level F' = 4 of the excited state, for

4

instance, may be considered for optical pumping and detection. The levels $F = 3$ and $F' = 2$, for instance, may be used for optical detection. It exists several such configurations, corresponding to a number of experimental arrangements.

In fact, the spectrum is even more complicated than shown in figure 2, because each hyperfine level has $2F + 1$ magnetic sublevels. In particular, the ground state has a total of sixteen sublevels which are equally populated at the atomic source exit.

The most simple experimental set-up is sketched in figure 3. A single semiconductor laser, at 0.852 μm, illuminates a cesium beam, on each side of the Ramsey microwave cavity. A population difference is created in the first light atom interaction region and the microwave transition is detected in the second one. In that set-up, one of the two hyperfine levels, $F = 3$ or 4 of the ground state is emptied to the benefit of the other one, if the light intensity is sufficiently large in the first interaction region. The population of the $F = 3$, $m_F = 0$ or of the $F = 4$, $m_F = 0$ sublevel, depending on the arrangement, becomes 1/8 of the total population of the beam. This is twice what may be expected with magnetic state selectors, which deflects off the beam one of these $m_F = 0$ levels. Figure 4 shows the microwave spectrum observed [8] with the experimental set-up of figure 3.

Another interesting consequence of the selection rules has been suggested by L. Cutler, pointed out by Lewis and Feldman [9] and theoretically investigated by de Clercq et al [10]. It affords the possibility to transfer the population of the sixteen hyperfine magnetic sublevels of the ground state to either the $F = 3$, $m_F = 0$ or the $F = 4$, $m_F = 0$ level. For instance, one light beam tuned to the $F = 3 \longleftrightarrow F' = 4$ transition will populate all the sublevels of the state $F = 4$. The second light beam, tuned on the $F = 4 \longleftrightarrow F' = 4$ transition will empty the sublevels of the state $F = 4$, with the exception of the sublevel $F = 4$, $m_F = 0$ because the transition $F = 4$, $m_F = 0 \longleftrightarrow F' = 4$, $m_F = 0$ is forbidden if the light is linearly polarized, parallel to the static field. It is then possible, in principle, to concentrate all the atoms on the $F = 4$, $m_F = 0$ level, for instance, whose population becomes 100 % of that of the beam. This major improvement has been experimentally achieved in two experimental configurations [8, 11]. In the first one, the detection is accomplished by a light beam derived from one pumping beam, and in the second one a third laser is used for the detection by a cycling transition. In figure 5, one sees that the field dependent $\Delta m_F = 0$ transitions have almost disappeared correspon-

ding to an increase of the central Rabi-Ramsey central line. Figure 6 shows the central Ramsey fringe obtained in a three lasers configuration.

b) Prospects

Besides the simplification in the design and the manufacturing of the cesium beam tube, optical pumping and detection methods have an impact on both the frequency stability and the accuracy of cesium beam frequency standards.

The short and medium term frequency stability measure, $\sigma_y(\tau)$, is determined by shot noise, for $\tau \lesssim 1$ day. It is approximately given by :

$$\sigma_y(\tau) \sim \frac{1}{Q} \frac{1}{(I\tau)^{1/2}} \tag{2}$$

where I is the flux of detected cesium atoms. The optical pumping method is able to make the most efficient use of the cesium beam :

- no atom is lost by velocity dependent magnetic deflection

- the atoms of the sixteen sublevels of the ground state can be accumulated on either the F = 3, $m_F = 0$ or the F = 4, $m_F = 0$ level

- wider beams may be used due to the absence of beam geometry limitations by magnet pole piece separation and hot wire detector width.

It is then very likely that the useful beam intensity I may be increased by a factor of the order of 100 and, thus,the frequency stability by a factor of about 10, so that a frequency stability figure approaching

$$\sigma_y(\tau) = 10^{-12} \tau^{-1/2} \tag{3}$$

appears feasible in manufactured units. Figure 7 compares this frequency stability with that of examples of presently manufactured cesium beam frequency standards. Among others, this achievement will require a suitable choice of the optical pumping and detection scheme and a proper design of the optical detection region in order to eliminate as well as possible spurious background light from the incident laser beam.

Systematic effects may also be greatly diminished, thereby improving the long term stability, reproducibility and accuracy

- the suppression of the field dependent side-bands of the microwave spectrum of the beam tube eliminates the frequency pulling by neighbouring lines [12]. As the separation between these side-bands depends on the applied static magnetic field, their absence allows to decrease its value and, consequently to decrease the sensitivity to ambiant magnetic field changes.

- the velocity distribution of the detected atoms is determined by the

interaction time with the light beams and the chosen method of optical detection. Well defined velocity distribution functions may be achieved [13], thus improving the knowledge of the second order Doppler effect.

- the absence of state selector magnets and the creation of a weak magnetic field all along the cesium beam cancel the probability of Majorana transitions, suppress the related frequency shift and ease the achievement of a better magnetic field uniformity.

- a better evaluation of the coupling between the velocity and the transverse position of atoms will enable a better averaging [14] of the transverse phase shift.

- the cesium beam may be designed symmetrical with an on-axis cesium oven at each end, thereby allowing a measurement and a correction of the cavity phase shift.

The light shift, which is inherent to optical methods is small here [15], because the optical and microwave interactions do not occur at the same place. It may be measured and kept constant to about one part in 10^{14}. As a consequence of a decrease, or a better control of systematic frequency shift, a frequency stability of the order of 1 x 10^{-14} may be expected over a year.

In addition, it is worth noting that it is of prime interest, from a fundamental point of view, to realize the S.I. time unit by significantly different means to verify that possible fundamental and apparatus effects have not been missed.

Use of slow atoms increase the line quality factor -which is inversely proportional to the velocity- and thus improve the short and medium term frequency stability (τ < 1 day) if the beam flux is not too much diminished. It also decreases the velocity dependent frequency shift and contributes to an increase of the long term frequency stability and to the accuracy. Slow atoms are already preferentially state selected in one of the primary cesium beam frequency standards [16]. In the same line, the interest in a fountain beam experiment [17] has been recently renewed [18]. Assuming that collisions do not scatter significantly the very slow atoms of a beam effusing from a properly designed over aperture, a possible accuracy of 10^{-15} has been anticipated for a machine, using 6 ms^{-1} optically pumped and detected Cs atoms.

Laser cooling is also studied [19,20], with the hope to produce intense and sufficiently well collimated beams of slow atoms.

3.2. Rubidium Beam Frequency Standard

One may consider the application of optical pumping and detection methods to a mass 87 rubidium beam [21], but using laser diode light sources instead of spectral lamps [6]. The wavelength of the D2 resonance transition, which is equal to 780 nm, is well suited, because it corresponds to that of light sources developed for the video-disc industry. However, besides that point, rubidium does not provide significant advantages for improved frequency standards.

- It has 8 hyperfine sublevels in the ground state, instead of 16 for cesium, but in both cases, then may be transferred to a single $m_F = 0$ by double wavelength optical pumping.

- Its mass is smaller than that of cesium. The line-width on the one hand and the velocity dependent frequency shift one the other hand would be slightly worse than for a cesium beam.

4. MAGNESIUM BEAM FREQUENCY STANDARD

As a consequence of their two valency electrons, earth alkaline atoms have singlet and triplet states. The ground state, $^1S_0$, is a singlet. The first triplet states, $^3P_{0,1,2}$, shown in the simplified energy diagram of Fig. 7, is metastable. The $^1S_0 \leftrightarrow {}^3P_0$ and the $^1S_0 \leftrightarrow {}^3P_2$ transitions are forbidden, for even isotopes, but the $^1S_0 \leftrightarrow {}^3P_1$ transition is slightly allowed. Consequently, a large population difference may be created between the ^3P fine structure levels by spontaneous decay of the $^3P_1$ level [4].

The fine structure splitting is rather large. The $^3P_1 \leftrightarrow {}^3P_0$ ones of Mg [22,23,24] and Ca are the smallest. They are given in Table 2, as well as the life time [25] of the $^3P_1$ level and the wavelength of the fluorescence light.

In a magnesium or a calcium beam frequency standard, the metastable $^3P_{0,1,2}$ levels are created in a discharge. At a distance downstream, which is of the order of 1 m for Mg, for instance, the population of the $^3P_1$ level is depleted by spontaneous decay. The dipole magnetic fine structure $^3P_0 \leftrightarrow {}^3P_1$ transition is induced in a sub-millimeter cavity, so that the level $^3P_1$ is replenished. The fine structure transition is then monitored by the intensity of the fluorescence light which is emitted by the beam, after its passage in the cavity. As usual, the resonance signal is processed to enable the frequency control of the interrogation frequency. Such a device, using a magnesium beam has been successfully operated [24], with a Rabi-type cavity at the present time.

8

With a Ramsey type sub-millimeter cavity, the short-term frequency capability of such a device would be [24] :

$$\sigma_y(\tau) = 3 \times 10^{-13} \ \tau^{-1/2} \tag{4}$$

for magnesium and 10 times better for calcium. This is mainly due i) to the high value of the line Q, of the order of 10^9, although limited by spontaneous decay of the $^3P_1$ level and ii) to the possibility to use wide atomic beams.

The very low sensitivity to magnetic fields and the absence of neighbouring transitions are positive points. But the long term stability, the reproducibility and the accuracy are limited to the 10^{-13} level by the second order Doppler effect [26] which is rather large due to the large velocity of light atoms forming a beam from a high temperature oven. It amounts to 2.5×10^{-12} for magnesium.

A magnesium beam machine must be several meters long to allow a sufficient decay of the $^3P_1$ level after the discharge region, and an efficient collection of the fluorescence light after the cavity. The length requirement is about 10 times less with Ca, according to the smallest life time of the $^3P_1$ level. The generation of the large interrogation frequency may cause technical problems.

5. RUBIDIUM CELL FREQUENCY STANDARDS

Spectral lamp optically pumped rubidium cell frequency standards are popular in applications where good short term stability, but relatively poor long term stability are compatible with small size, small power consumption and low cost.

A buffer gas is introduced in the cell containing mass 87 rubidium atoms to enhance the optical pumping efficiency [27]. Nitrogen quenches rubidium atoms in the excited state so that they make a non radiative transition to the ground state. Otherwise, the fluorescence light, which contains both hyperfine components, would decrease the attained population difference. In addition, the slow diffusion of atoms in the buffer gas greatly reduces the Doppler broadening [28], without requirement on the size of the cell compared to the microwave wavelength, so that the Doppler free hyperfine transition can be observed with a cell filling the microwave cavity ※.

※ In that case, the microwave cavity is not necessary. This Doppler free trandition may be observed if the cell is placed in a travelling wave at the hyperfine transition frequency.

With a laser light source the optical pumping efficiency is highly increased, due to the much larger energy density at the proper wavelength. It would then be possible to suppress the buffer gas, provided i) that the cell does not extend to regions where the phase of the standing microwave magnetic field is reversed and ii) that a wall coating prevents strong relaxation on the glass wall. The great advantage would be the elimination of the large size buffer gas frequency shift and,mainly,of the inhomogeneous line broadening effects causing large power frequency shifts [28bis] due to the absence of motional averaging when a buffer gas is used. These inhomogeneous line broadening effects are produced by the progressive absorption of light along its path in the cell, causing a distributed light shift, and by inhomogeneous magnetic field. In that event, the buffer gas frequency shift would be replaced by a noticeably smaller wall shift.

One may then expect that the larger resonance signal increases the short term frequency stability and that the reduction of frequency offsets improves the medium and long term frequency stability. This assumes i) that the optical wavelength is tuned to that of the D_2 line, so that the light shift goes to zero and ii) that the amplitude and frequency noises [29] of the laser is sufficiently reduced so that they are not transduced into fluctuations of the frequency of the hyperfine transition. In the event that these requirements cannot be fulfilled, it would be possible to eliminate light shift related effects by performing sequential optical pumping and by observing hyperfine transition "in the dark".

Optical pumping of the rubidium maser by diodes may be considered as well, but with the same limitations.

6. THE HYDROGEN MASER

6.1. Standard Size Hydrogen Maser

The standard size hydrogen maser usually includes a TE_{011} microwave cavity, resonating at 1.42 GHz, with a thin walled teflon coated storage quartz bulb. A typical size is 12 x 7.7 x 5.3 dm^3. The device is able to sustain a self-oscillation, so that it is said active.

The standard size hydrogen maser is the most stable atomic frequency standard [30], as shown in Fig. 9. The medium term frequency stability 10 s $< \tau <$ 1 hour is determined by the thermal noise in the microwave cavity. We have :

$$\sigma_y(\tau) = K_1 \frac{1}{Q} \left(\frac{kT}{2P\tau}\right)^{1/2} \tag{5}$$

where k is Boltzman constant, T the absolute temperature of the cavity, Q the atomic line-width and P the power delivered to the microwave cavity by the hydrogen atoms. K_1 is unity for active masers. An optimization of the operating parameters is possible [31] but would only improve very slightly the frequency stability, as shown in Fig. 10.

Short term frequency stability ($\tau < 10$ s) is mainly determined by the noise added in the first stage of the microwave receiver. We have, approximately :

$$\sigma_y(\tau) = K_2 \left(\frac{kT}{P}\right)^{1/2} \frac{1}{\tau} \tag{6}$$

T is the noise temperature of the receiver and K_2 is a constant which depends on the noise bandwidth.

The long term frequency stability ($\tau > 1$ hour) is determined by environmental effects, which are mainly related to the cavity pulling effect [32,33]. If necessary, it would be possible to operate a fast autotuning system [34] to keep the resonant frequency of the cavity under control, thereby improving the long term frequency stability figure to values of the order of 10^{-15} without degrading the short and medium term stability.

The accuracy of the hydrogen maser is still limited by the lack of reproducibility of the wall shift. The best achieved accuracy [35] is 6 x 10^{-13} in a standard size maser. It seems difficult to improve it with teflon coatings. However, this is better than the accuracy and the reproducibility of presently manufactured cesium beam frequency standards. This does not cause serious problems in the main fields of application of the standard size hydrogen maser i.e. : very long base line radio-interferometry and navigation.

6.2. Small Size Hydrogen Masers

The key of size reduction is a decrease of the microwave cavity dimensions, its resonance frequency being kept equal to 1.42 GHz. This is achieved by using properly disposed dielectric materials [36] or conductors [37,38] as shown in Fig. 11. The achieved size of the maser is then of the order of 6 x 5 x 3.5 dm^3. However, the presence of materials in the cavity increases the losses and the quality factor becomes smaller than 10 000, which does not enable self-oscillation to occur anymore. The small size hydrogen masers may then be operated in two different ways : either passively [39] or actively [40]. In the last case, electronic feedback is used to enhance the cavity quality factor above oscil-

11

lation threshold. In both circumstances, the frequency stability is given by Eq. 5, but with K_1 larger than unity. The achieved frequency stability is very good [41][42]. Fig. 12 shows the result obtained with a passively operated small size hydrogen maser of a particular design. The short and medium term frequency stability may still be improved by proper optimization of the operating parameters [31], as shown in Fig. 10. The long term stability happens to be excellent [42], of the order of 3×10^{-15} for $\tau = 10$ days, although the thermal coefficient of the loaded cavity is large. This shows that the achieved long term stability is due to the operation of an efficient electronic control of the cavity.

Actually, the small size hydrogen maser realizes an excellent trade-off between performance and size.

6.3. Cold Hydrogen Maser

The interest to cool the hydrogen maser has been recognized early in the history of this device. It was motivated by two different but complementary reasons : i) since the achieved short and medium term frequency stability is determined by thermal noise, cooling must improve the short and medium term stability [43], as shown by Eq. 5 and 6 and ii) cooling provides a means of studying the properties of the wall coating [44,45] and to search for materials having more reproducible properties than teflon at room temperature. In that respect, the following materials have been studied : FEP 120 teflon down to 48 K [44-46] and tetrafluoromethane between 50 and 25 K [47].

At approximately the same time, fundamental studies aimed to achieve Bose-Einstein condensation of hydrogen atoms in a high density gas of spin polarized hydrogen atoms were engaged in several laboratories. This led to information on the interaction of hydrogen atoms with molecular hydrogen surfaces around 4 K [49,50]. A very significant breakthrough occured when it was discovered that ^{3}He and ^{4}He films are able to contain a high density of polarized hydrogen gas below 1 K [51].

This result opens very promising prospects for a cryogenic hydrogen maser frequency standard, for the following reasons, pointed out by Berlinsky and Hardy [52] :

- the binding energy of H on a ^{3}He or a ^{4}He surface is 0.4 K or 1.15 K, respectively, thus allowing low enough recombination rates at the surface at temperatures below 1 K.

12

- the total pressure shift in the gas plus wall shift shows a minimum around 0.2 K for ^{3}He and 0.5 K for ^{4}He. The frequency shift in a 15 cm diameter storage bulb is then of the same magnitude than with teflon at room temperature.

- the helium film is homogeneous and of high purity, and the pressure of the helium gas can be controlled well enough to expect a fractional frequency stability of the order of 10^{-18}.

- the spin exchange line broadening effect is 10^3 times smaller at very low temperature than at room temperature. This allows larger oscillation power to be obtained.

- the cavity pulling effect should be drastically reduced because materials have a very low expansion coefficient at low temperature and because it is possible to operate the cold maser at low values of the cavity quality factor.

- slow hydrogen atoms issued from a cold hydrogen source may be very easily state selected.

- magnetic shielding may be provided by superconductive materials.

- cooled GaAs FET amplifiers are available with noise temperature of 10 K.

From these statements, a fractional frequency capability of 2×10^{-18} for $\tau > 10^3$ s is anticipated [52]. One may add that the pressure and the wall shift been assumed reproducible, the accuracy should be very significantly increased too.

However difficulties arise, which are related to the background pressure of ^{4}He at 0.5 K, for instance, giving a mean free path of 1.4 cm. A means to introduce the hydrogen gas in the storage cell should be found. In addition, the motional averaging effect occuring in conventional hydrogen masers disappears which may cause severe requirements on the magnetic field homogeneity.

7. ION STORAGE

It is known, since several tens years that one may store charged particles in electric and magnetic fields [53] (Penning trap) or in a radiofrequency electric field [54] (r.f. trap). Storage may occur for hours, and the interest of this technique for high resolution -microwave spectroscopy, of ^{3}He$^+$ at first, has been demonstrated by Dehmelt [55].

It has been proved that it is possible to use a hyperfine structure transition, that of the mass 199 mercury ion, to realize an experimental model of a fre-

quency standard using ions stored in a radiofrequency trap [56-59].

In the following we shall mainly focus on the radiofrequency trap and the mercury ions frequency standard and we shall give indications on the potentialities of stored cooled ions [60].

7.1. Storage in a r.f. Trap

Let us consider the three electrodes system and the applied voltage shown in Fig. 13. Assuming that the electrodes have the proper hyperboloïd shape, the axial and transverse components of the electric field are proportional to the distance from the center O of the trap, but they have opposite signs. If the voltage is a constant, a charged particle will be submitted to a repulsive force either in the axial or the transverse direction, according to its sign, and no storage may occur.

The situation is different if the voltage is alternating, with frequency v_c. The electric field forces a motion at the frequency v_c, whose amplitude is small. It is called the micromotion. This motion is approximately sinusoïdal. As shown in Fig. 14, the axial and transverse micromotions are out of phase because the two components of the electric field have opposite signs. In its motion, the particle explores the electric field and, due to its non-uniformity, the acting electric force is not sinusoïdal. It follows that it has a non zero mean value and it may be shown that its two components tend to attract the particle towards the center of the trap. This central force imposes another harmonic motion of larger amplitude called the secular motion. Its frequency v_s is in general noticeably smaller than v_c. If the inner dimensions of the trap are of the order of 1 cm, v_c equals 200 kHz and has an amplitude of 100 V, then v_s is of the order of 20 kHz for the mercury ion and the amplitude of the macromotion is of the order of a few mm. Therefore, within conditions [61] which have not been considered here, the charged particle motion has a finite amplitude and the particle may stay inside the trap for very long times, provided that it does not suffer collisions with the background gas. It is worth noting that a stored ion cloud is very dilute as a consequence of the Coulomb repulsive forces leading to the so-called space charge effect. Usually the ion density is limited to about 10^6 per cubic centimeter.

Assume now that the ions are irradiated by an electromagnetic wave at frequen-

cy ν_o. According to their harmonic motion, they will see a Doppler frequency modulated wave composed of a carrier at frequency ν_o and side-bands separated by ν_s, at least, from the carrier. If the ion atomic spectrum has a sharp line close to the frequency ν_o, only the carrier component of the wave will be effective and the condition of high resolution Doppler free spectroscopy is met.

These principles are implemented in the mercury ion frequency standard, for instance.

7.2. The Mercury Ion Frequency Standard

The mass 199 mercury ion has a hyperfine structure in the ground state shown in Fig. 15. One has $I = 1/2$, and the hyperfine structure is as simple as that of the hydrogen atom, but the hyperfine separation is large, equal to about 40.5 GHz (see Table 1). The hyperfine transition is observed by conventional optical pumping techniques owing to a favorable isotope shift of the mass 202 mercury ion. The experimental set-up is shown in Fig. 16. A lamp filled with ^{202}Hg emits the resonance light of the ionized mercury at 194 nm. This light is selectively absorbed by those stored ^{199}Hg$^+$ ions which are in the $F = 1$ hyperfine level. This level is depopulated to the benefit of the $F = 2$ level and the intensity of the fluorescence light is weak. If now the microwave transition at 40.5 GHz is induced, the level $F = 1$ is replenished and the intensity of the fluorescence light increases. This intensity is used to monitor the microwave hyperfine transition. Fig. 17 shows a power broadened hyperfine resonance pattern, corresponding to a line quality factor of 5 x 10^9. The high value of the quality factor compensates for the relatively poor signal to noise ratio. A quartz crystal frequency source has been frequency locked on such a transition and a short term frequency stability (10 s $< \tau <$ 3500 s) of

$$\sigma_y(\tau) = 3.6 \ 10^{-11} \tau^{-1/2} \tag{7}$$

has been obtained [58]. It is shown in Fig. 18.

A substantially narrower line, 0.85 Hz wide, has been achieved, in a different set-up [59,62] where the light broadening and frequency shift are eliminated by switching off periodically the pumping light and by interrogating the microwave transition in the dark.

Stored ions have a relatively large kinetic energy of about 1 eV and, conse-

quently a large second order Doppler shift, of $\sim 5 \times 10^{-12}$ per eV in the case of mercury. Models for the effect of the ion number, i.e. of the space charge effect on the ion motion and the ion kinetic energy have been established [62,63]. This has led to a measurement of the ion kinetic energy [63] and to the extrapolation to zero Doppler shift of the hyperfine transition frequency in a mercury ion cloud cooled by viscous drag with helium [62]. The cooling gas is efficient under very low pressure, of the order of 10^{-5} Torr, for which the pressure shift is about 6×10^{-14}.

The short and medium term capability of the mercury ion frequency standard is of $10^{-12}\,\tau^{-1/2}$ about [62,64]. A long term frequency stability of 2.2×10^{-14} and an accuracy of 2.5×10^{-13} are anticipated.

The mercury ion frequency standard can be built smaller than the presently manufactured cesium beam frequency standard. It is then a potential competitor of this device. However, technical problems related to the life-time of the $^{202}Hg^{+}$ lamp and to the control of the pressure of the background neutral mercury remains to be solved.

7.3. Microwave Spectroscopy in Radiofrequency Traps

The ground state hyperfine splitting of several ionized elements has been measured, with a precision of the order of 10^{-10} using the r.f. trap storage technique and a pulsed dye laser for optical pumping. They are $^{135}Ba^{+}$ (493 nm) at 7.18 GHz [65], $^{137}Ba^{+}$ (493 nm) at 8.04 GHz [66] and $^{171}Yb^{+}$ (369 nm) at 12.6 GHz [67], where the quantity within parenthesis is the wavelength used for optical pumping. A fractional linewidth up to 3.8×10^{11} has been obtained in such experiments, which shows their interest in the field of atomic frequency standards. An experimental set-up has been realized in which a quartz crystal oscillator has been frequency locked to the hyperfine transition of $^{137}Ba^{+}$ [68]. However, the drawback of these devices, compared to the mercury ion frequency standard is the requirement of a pulsed dye laser, at least at the present time.

7.4. Ion Cooling

In the absence of any collision, stored ions have an agitation energy which is larger than the room temperature thermal energy, especially in r.f. traps. As stated previously, collisions with the atoms of a rarefied light gas are

efficient to thermalize ions [67,69,70], in a r.f. trap with the additional benefit of an increase of the stored ion number and of their storage time.

However, the most efficient cooling is by means of side-band laser irradiation [71,72] which takes advantage of the Doppler effect. A schematical explanation is the following. Due to the harmonic motion in a trap, the absorption spectrum of the stored ions shows lower and upper sidebands. An ion can absorb a photon whose frequency, ν_L coincides with a component of the lower sideband. We then have $\nu_L < \nu_0$, where ν_0 is the transition frequency of the ion at rest. By spontaneous emission, the excited ion will emit a photon, with the frequency ν_0 in the average. In that process the ion looses the energy $h(\nu_L - \nu_0)$ which decreases its kinetic energy. This process requires an ion having a short life time of the excited level in order to enable a large number of such cycles every second. Efficient cooling has been demonstrated, using Mg^+ ions, either in a Penning trap [73,74] or a r.f. trap [75], or using Ba^+ ions in a r.f. trap [76]. Temperatures as low as 5 mK have been observed with a single stored Mg^+ ion [75]. Due to zero point energy, the lowest attainable temperature is of the order of

$$T = \frac{1}{2} \hbar \gamma / k \tag{8}$$

where γ is the natural linewidth of the transition. Typically, we have $T = 1$ mK.

One of the most impressive recent achievement has been the observation and the spectroscopy of single stored cooled Mg^+ [75,77] and Ba^+ ions [78].

7.5. Frequency Standards with Cooled Stored Ions

Precision microwave spectroscopy of $^{25}Mg^+$ [79] and $^9Be^+$ [80] ions confined in a Penning trap and laser cooled has been accomplished. In that experiments the magnetic field was stabilized to a value for which some of the hyperfine transitions show a minimum.

Following these experiments, a laboratory microwave frequency standard using $^9Be^+$ ions has been investigated [81]. Approximately 300 ions are stored in a Penning trap at a magnetic field of 0.82 T and laser cooled with a laser beam at a wavelength of 313 nm This laser beam is produced from the output of a single mode dye laser by the frequency doubling technique, in a non linear crystal. Although the transition frequency is small, equal to approximately

17

300 MHz, in that experiment, the very long storage time enabled to achieve a line-width as small as 10 mHz, and a line quality factor of 1.2×10^{10} has thus been obtained. A quartz crystal oscillator locked to a transition of the hyperfine manifold has a frequency stability given by :

$$\sigma_y(\tau) = 2 \times 10^{-11} \tau^{-1/2} \tag{9}$$

for 400 s $< \tau <$ 3200 s, of the same order as achieved in manufactured cesium beam frequency standards. The magnetic field instability contributes an uncertainty of 3×10^{-14} in this experiment and the second order Doppler shift is $- 5 \times 10^{-14}$ only, due to the cooling.

7.6. Prospects

Ion storage in a r.f. trap or a Penning trap has proved to be a promising technique for frequency standard applications. The r.f. trap is best suited to the realization of a portable clock. Laser cooling affords the possibility of a drastic reduction of velocity dependent frequency shifts, and of the most annoying of them, the second order Doppler frequency shift. In addition, the related very small spatial extension of the ion motion reduces the effects of magnetic field homogeneïty, accordingly. However, laser cooling is tributary upon suitable coherent c.w. light sources adapted to ions having a favorable energy level diagram, and it can be contemplated for laboratory frequency standards only. In that respect, a mass 201 mercury ion frequency standard is being studied [82]. The required wavelength, at 194 nm has been coherently produced [83]. A frequency stability better than $10^{-16} \tau^{-1/2}$ and an accuracy better than 10^{-15} are expected. Another similar proposal refers to the use of $^{137}Ba^+$ [84].

Although this is out of the scope of this paper, it should be mentionned that laser cooled stored ions are being considered for optical frequency standards [85,86]. At optical frequencies, which are roughly 10^4 times larger than microwave frequencies, the line quality factor and, therefore the performances should be greatly enhanced. The most fascinating proposal is by Dehmelt [87]. He considers a single ion stored in a r.f. trap, such as the $^{205}Tl^+$ ion whose spectrum contains both a wide line and a very narrow line sharing in common one energy level. The very narrow line is used as the frequency reference feature. The broad line, corresponding to a short-lived excited state is used for efficient laser cooling and as a cycling transition providing about 10^6

18

photons each time the narrow line transition is induced. This yields an optical resolution capability of 1 part in 10^{18}. However, optical frequency generation and synthesis must be greatly improved, mainly in the UV part of the spectrum before such a potentiality can be experimentally verified.

8. CONCLUSION

It then appears that the performances of atomic frequency standards are open to significant improvement. Table 3 summarizes the potentialities[*] of some of the considered devices.

The cold hydrogen maser and the cooled trapped ions frequency standards using storage techniques show the best promise of frequency stability improvement. In a trap the storage process does not involve collisions either with a wall or a buffer gas. For cooled ions, almost at rest at the center of the trap, the confinement related frequency shifts are either extremely small (effect of the electric field) or calculable with a great precision (effect of the magnetic field). It follows that the expected accuracy is impressively good. The cold hydrogen maser and the cooled trapped ions frequency standards will be suited to applications in the field of fundamental research (experimental verification of Relativity theories, search for gravitational waves), to deep space navigation or to fundamental metrology.

Other devices such as the optically pumped portable cesium beam frequency standard, the small size hydrogen maser, the mercury ion frequency standard and the rubidium frequency standard have frequency stability capabilities very significantly better than achieved at present. They will remain of moderate size and cost and they will certainly find a number of technical applications such as in navigation systems.

It is worth reminding that application of optical methods to laboratory primary cesium beam frequency standards is being studied in a number of laboratories. This is of prime importance to verify that two different designs of the realization of the definition of the time unit, one using magnetic state selection and the other optical pumping and detection methods, yields the same result.

---

[*] *The author is not familiar enough with Rb clocks to give pertinent figures for this device.*

REFERENCES

(1) J.A. Barnes, A.R. Chi, L.S. Cutler, D.J. Healey, D.B. Leeson, T.E. Mc Gunigal, J.A. Mullen Jr., W.L. Smith, R.L. Sydnor, R.F.C. Vessot and G.M.R. Winkler, Proc. IEEE Trans. on Instr. and Meas. IM-20 (1971) p. 105

(2) H. Hellwig, Proc. of the IEEE 63 (1975) p. 212

(3) C. Audoin and J. Vanier, Journal de Physique E, Scientific Instruments 9 (1976) p. 697

(4) F. Strumia, Metrologia 8 (1972) p. 85

(5) A. Kastler, J. de Physique et le Radium 11 (1959) p. 255

(6) P. Cerez, M. Arditi and A. Kastler, Comptes-Rendus Acad. Sci. 267B (1968) p. 282

(7) M. Arditi and J.L. Picqué, J. de Physique Lettres 41 (1980) p. L-379

(8) G. Avila, E. de Clercq, M. de Labachelerie and P. Cérez, Conference on Precision Electromagnetic Measurement. Delft, the Netherlands, 1984

(9) L.L. Lewis and M. Feldmann, Proc. of the 35th Annual Frequency Control Symposium, Philadelphia, USA (1981), p. 612

(10) E. de Clercq, M. de Labachelerie, G. Avila, P. Cérez and M. Têtu, J. de Physique 45 (1984) p. 239

(11) E. de Clercq, G. Avila, M. de Labachelerie, P. Petit and P. Cérez, Congrès International de Chronométrie, Besançon, France, 1984

(12) A. de Marchi, G.D. Rovera and A. Premoli, Metrologia 20 (1984) p. 37

(13) P. Cérez, G. Avila, E. de Clercq, M. de Labachelerie and M. Têtu, Proc. of the 38th Annual Symposium on Frequency Control, Philadelphia, USA (1984)

(14) S. Jarvis, Jr., Metrologia 10 (1974) p. 87

(15) A. Brillet, Metrologia 17 (1981) p. 147

(16) G. Becker, IEEE Trans. on Instr. and Meas. IM-27 (1978) p. 319

(17) J.R. Zacharias, Phys. Rev. 94 (1954) p. 751

(18) A. de Marchi, Metrologia 18, (1982), p. 103

(19) J.V. Prodan, W.D. Philipps and H. Metcalf, Phys.Rev. Lett. 49 (1982) p. 1149

(20) V.O. Balykin, V.S. Letokhov and A.I. Sidorov, Optics Com. (1984) p. 248

(21) M. Feldmann, J.C. Bergquist, L.L. Lewis and F.L. Walls, Proc. of the 35 th Annual Frequency Control Symposium, Philadelphia, USA (1981) p. 625

(22) A. Godone, A. de Marchi, G.D. Rovera and E. Bava, Phys. Rev. A, 28 (1983) p. 2562

(23) E. Bava, A. de Marchi, A. Godone, G.D. Rovera and G. Giusfredi, Optics Com. 47 (1983) p. 193

(24) A. Godone, E. Bava, A. de Marchi, G.D. Rovera and G. Giusfredi, 21st General Assembly of URSI, Firenze, Italy (1984)

(25) H.S. Kwong, P.L. Smith and W.H. Parkinson, Phys. Rev. A, 25 (1982) p.2629

(26) A. de Marchi, E. Bava, A. Godone and G. Giusfredi, IEEE Trans. on Instr. and Meas. IM-32 (1983) p. 191

(27) P. Davidovits and R. Novick, Proc. of the IEEE 54 (1966) p. 155

(28) R.H. Dicke, Phys. Rev. 89 (1953) p. 472

(28bis) A. Risley, S. Jarvis Jr and J. Vanier, Proc. of the 33rd Annual Symposium on Frequency Control, Atlantic City, USA (1979) p. 477

(29) L.L. Lewis and M. Feldman, Proc. of the 35th Annual Frequency Control Symposium, Philadelphia, USA, (1981) p. 612

(30) M.W. Levine, R.F.C. Vessot and E.M. Mattison, Proc. of the 32nd Annual Symposium on Frequency Control, Atlantic City, USA (1978), p. 477

(31) C. Audoin, J. Viennet and P. Lesage, Journal de Physique 42 , Supplément au n° 12 (1981) p. C8-159

(32) D. Kleppner, H.M. Goldenberg and N.F. Ramsey, Phys. Rev. 126 (1962) p. 603

(33) D. Kleppner, H.C. Berg, S.B. Crampton, N.F. Ramsey, R.F.C. Vessot, H.E. Peters and J. Vanier, Phys. Rev. A 138 (1965) p. 972

(34) C. Audoin, Revue de Physique Appliquée 16 (1981) p. 125 and 17 (1982) p. 273
also : H.E. Peters, Proc. of the 36th Annual Frequency Control Symposium, Philadelphia, USA (1982) p. 240

(35) P. Petit, M. Desaintfuscien and C. Audoin, Metrologia 16 (1980) p. 7

(36) D.A. Howe, F.L. Walls, H.E. Bell and H. Hellwig, Proc. of the 33rd Annual Symposium on Frequency Control, Atlantic City, USA (1979) p. 554

(37) H.E. Peters, Proc. of the 32nd Annual Frequency Control Symposium, Atlantic City, USA (1978) p. 469

(38) H.T.M. Wang, J.B. Lewis and S.B.Crampton, Proc. of the 33rd Annual Symposium on Frequency Control, Atlantic City, USA (1979) p. 543

(39) F.L. Walls and H. Hellwig, Proc. of the 39th Annual Symposium on Frequency Control, Atlantic City, USA (1978) p. 473

(40) H.T.M. Wang, Proc. of the 34th Annual Symposium on Frequency Control, Philadelphia, USA (1980) p. 364

(41) H.T.M. Wang, Proc. of the 36th Annual Symposium on Frequency Control, Philadelphia, USA (1982), p. 249

(42) F.L. Walls and K.B. Persson, Proc. of the 38th Annual Frequency Control Symposium, Philadelphia, USA (1984) p. 416

(43) R.F.C. Vessot, M.W. Levine and E.M. Mattison, Proc. of the 9th Annual PTTI. Applications and Planning Meeting, Greenbelt, USA (1978), p.549

(44) P.W. Zitzewitz and N.F. Ramsey, Phys. Rev. A $\underline{3}$ (1971) p. 51

(45) M. Desaintfuscien, J. Viennet and C. Audoin, Metrologia $\underline{13}$ (1977) p. 125

(46) R.F.C. Vessot, E.M. Mattison and E. Imbier, Proc. of the 37th Annual Symposium on Frequency Control, Philadelphia, USA (1983) p. 49

(47) R.F.C. Vessot, E.M. Mattison and E.L. Blomberg, Proc. of the 33rd Annual Symposium on Frequency Control, Atlantic City, USA (1979), p. 511
also : R.F.C. Vessot, E.M. Mattison, E. Imbier and Z.C. Zhai (1984), this conference

(48) S.B. Crampton, K.M. Jones, G. Nunes and S.P. Souza (1984), this conference

(49) S.B. Crampton, J.J. Krupczak and S.P. Souza, Phys. Rev. B $\underline{25}$ (1982) p. 4383

(50) W.N. Hardy, A.J. Berlinsky and L.A. Whitehead, Phys. Rev. Lett $\underline{42}$ (1979) p. 1042

(51) W.N. Hardy and M. Morrow, Journal de Physique, $\underline{42}$, supplément C8 (1981) p. 171 and quoted references

(52) A.J. Berlinsky and W.N. Hardy, Proc. of the 13th Annual PTTI. Applications and Planning Meeting, Washington D.C., USA (1981) p. 547

(53) F.M. Penning, Physica $\underline{3}$ (1936) p. 873

(54) W. Paul, O. Osberghaus and E. Fischer, Forschungber. Wirtsch. Verkehrs-ministerium Nordrhein-Westfalen n° 415 (1958)

(55) H.G. Dehmelt in Advances Atomic and Molecular Physics $\underline{3}$ (1967) p. 53 and $\underline{5}$ (1969) p. 109

(56) F.G. Major and G. Werth, Phys. Rev. Lett. $\underline{30}$ (1973) p. 1155

(57) M.D. Mc Guire, R. Petsch and G. Werth, Phys. Rev. A $\underline{17}$ (1978) p. 1999

(58) M. Jardino, M. Desaintfuscien and C. Audoin, Applied Physics $\underline{24}$ (1981) p. 167

(59) L.S. Cutler, R.P. Giffard and M.D. Mc Guire, Proc. of the 13th Annual PTTI. Applications and Planning Meeting, Washington, D.C., USA (1981), p. 563

(60) D.J. Wineland, Proc. of the 13th Annual PTTI. Applications and Planning Meeting, Washington D.C., USA (1981) p. 579

(61) F.G. Major and H.G. Dehmelt, Phys. Rev. $\underline{170}$ (1968) p. 91

(62) L.S. Cutler, R.P. Giffard and M.D. Mc Guire, Proc. of the 37th Annual Frequency Control Symposium, Philadelphia, USA (1983) p. 32

(63) M. Jardino, F. Plumelle, M. Desaintfuscien and J.L. Duchêne, Proc. of the 38th Annual Frequency Control Symposium, Philadelphia, USA (1984) p. 431

(64) M. Jardino, M. Desaintfuscien and F. Plumelle, Journal de Physique $\underline{42}$ Supplément au n° 12 (1981) p. C8-327

(65) W. Becker and G. Werth, Zeits.. für Physik A, $\underline{311}$ (1983) p. 41

(66) R. Blatt and G. Werth, Phys. Rev. A $\underline{25}$ (1982) p. 1476

(67) R. Blatt, H. Schnatz and G. Werth, Zeits. für Physik A $\underline{312}$ (1983) p. 143

(68) H. Knab, K.D. Niebling and G. Werth, Conference on Precision Electromagnetic Measurement, Delft, the Netherlands (1984)

(69) J. André and F. Vedel, Journal de Physique $\underline{38}$ (1977) p. 1381

(70) F. Plumelle, M. Desaintfuscien, J.L. Duchêne and C. Audoin, Optics Com. $\underline{34}$ (1980) p. 71

(71) D.J. Wineland and W.M. Itano, Phys. Rev. A $\underline{20}$ (1979) p. 1521 and quoted references

(72) D.J. Wineland and W.M. Itano, Phys. Rev. A $\underline{25}$ (1982) p. 35 and quoted references

(73) D.J. Winaland and R.E. Drullinger, Phys. Rev. Lett. $\underline{40}$ (1978) p. 1639

(74) F. Plumelle, private communication (1984)

(75) W. Nagourney, G. Janik and H. Dehmelt, Proc. Natl. Acad. Sci. (USA) $\underline{80}$ (1983) p. 643

(76) W. Neuhauser, M. Hohenstatt, P. Toschek and H. Dehmelt, Phys. Rev. Lett. $\underline{41}$ (1978) p. 233

(77) W. Neuhauser, M. Hohenstatt and P.E. Toschek, Phys. Rev. A $\underline{22}$ (1980) p. 1137

(78) D.J. Wineland and W.M. Itano, Physics Letters 82A (1982) p. 75

(79) W.M. Itano and D.J. Wineland, Phys. Rev. A 24 (1982) p. 1364

(80) J.J. Bollinger, D.J. Wineland, W.M. Itano and J.S. Wells in Laser
Spectroscopy VI. Springer series optical sciences 4, p. 168

(81) J.J. Bollinger, W.M. Itano and D.J. Wineland, 37th Annual Frequency
Control Symposium, Philadelphia, USA (1983) p. 37

(82) D.J. Wineland, W.M. Itano, J.C. Bergquist and F.L. Walls, Proc. of the
35th Annual Symposium on Frequency Control, Philadelphia, USA (1981)
p. 602

(83) H. Hammati, J.C. Bergquist and W.M. Itano, Optics Letters 8 (1983) p. 73

(84) F.L. Walls, D.J. Wineland and R.E. Drullinger, Proc. of the 32nd Annual
Frequency Control Symposium, Atlantic City, USA (1978) p. 453

(85) P.L. Bender, J.L. Hall, R.H. Garstang, F.M.J. Pichanick, W.W. Smith,
R.L. Barger and J.B. West, Bulletin Am. Phys. Soc. 21 (1976) p. 599

(86) D.J. Wineland, W.M. Itano and R.S. Van Dyck Jr. in Advances in Atomic and
Molecular Physics 19, Academic Press (1983) and quoted references

(87) H.G. Dehmelt, IEEE Trans. on Instr. and Meas. IM-31 (1982) p. 83

	ν_0	$\Delta\nu_1/\nu_0$	$\Delta\nu_2/\nu_0$
^{133}Cs	9 192 631 770 Hz	-2.45×10^{-20} E^2	4.64 B^2
^{1}H	1 420 405 751.770 $\pm$ 0.003 Hz∷	-5.5×10^{-23} E^2	195.3 B^2
^{87}Rb	6 834 682 612.8 $\pm$ 0.5 Hz	-1.8×10^{-20} E^2	8.42 B^2
^{199}Hg$^+$	40 507 347 996.9 $\pm$ 0.3 Hz	-3×10^{-22} E^2	0.24 B^2

TABLE 1. Property of the hyperfine transition of some elements. ν_c is the hyperfine transition frequency, expressed in Hz. $\Delta\nu_1$ and $\Delta\nu_2$ are the Stark frequency shift and the Zeeman frequency shift, respectively. E is expressed in Volt per meter and B in Tesla.

∷ *Mean value of measurements in which the wall frequency shift has been measured at the same time as the hydrogen hyperfine transition frequency and in which the measurement uncertainty of the unperturbed transition of hydrogen was smaller than 4×10^{-3} Hz.*

	ν_o[Hz]	τ[ms]	λ[nm]
^{24}Mg	601. 27715833 (20)	4.6	457.1
^{26}Mg	601. 278866 (4)	4.6	457.1
^{40}Ca	1563. 6	0.55	657.3

TABLE 2. Property of fine structure transitions in magnesium and calcium. ν_o is the frequency of the $^3P_1 \longleftrightarrow {}^3P_0$ fine structure transition, τ is the life-time of the $^3P_1$ level and λ is the wavelength of the $^3P_{1,2,3} \to {}^1S_0$ fluorescence light.

Device	Short and medium term frequency stability	Accuracy	Possible technical difficulty
Optically pumped Cs (portable)	$10^{-12} \tau^{-1/2}$ 10^{-14} (year)	10^{-13}	Reliability of laser diodes
Small size H maser	$3 \times 10^{-13} \tau^{-1/2}$	10^{-12}	
Cold H maser	$\left[(2.9 \times 10^{-17} \tau^{-1/2})^2 + (1.2 \times 10^{-16} \tau^{-1/2})^2\right]^{1/2}$	$10^{-13}/10^{-14}$	Refrigeration, injection of atoms in the storage cell
Mg beam	$3 \times 10^{-13} \tau^{-1/2}$	10^{-13}	Sub-millimeter frequency source
$^{199}Hg^+$	$10^{-12} \tau^{-1/2}$	10^{-13}	Life time of lamp, control of neutral mercury pressure
Cooled ions ($^{201}Hg^+$)	$10^{-16} \tau^{-1/2}$	10^{-15}	Cooling laser source

TABLE 3. Summary of the potentialities of some atomic frequency standards.
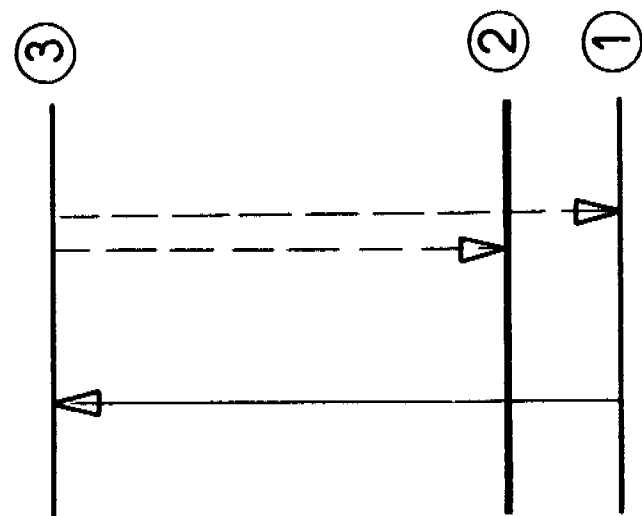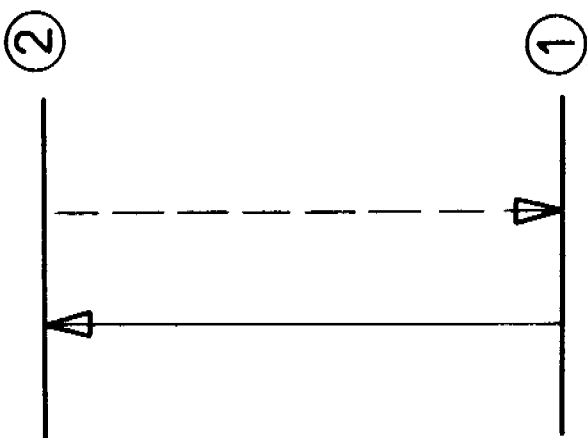
Optical Pumping   Optical Detection

Schematic representation of optical pumping and detection methods.

Fig.1
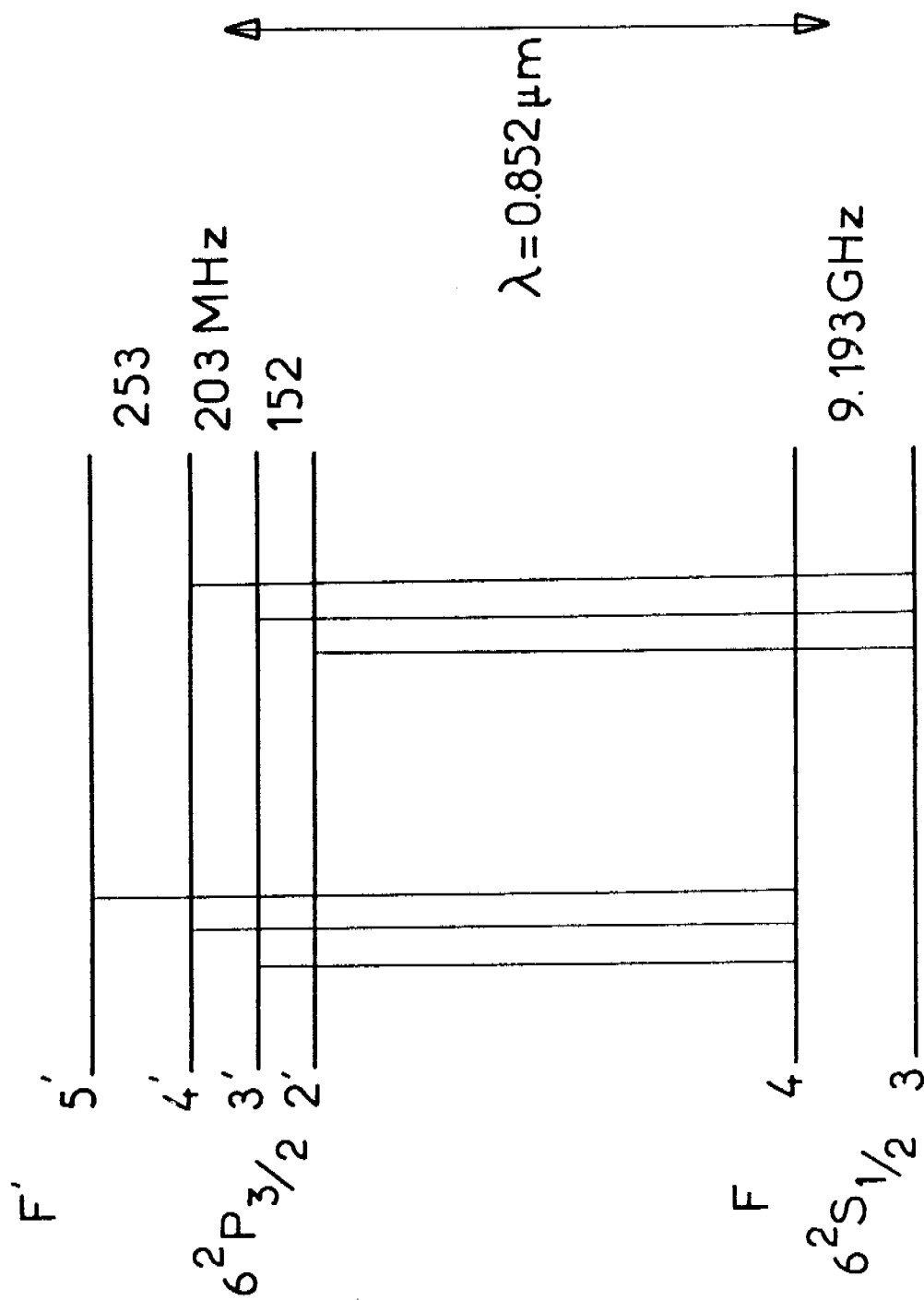
Fig.2

Simplified energy diagram of the cesium atom, with the hyperfine structure of the $6^2S_{1/2}$ ground state and of the $6^2P_{3/2}$ second excited state. Magnetic sub-levels are not shown. Vertical lines represent allowed transitions.

Optical
Detection
Region

9.193GHz

Ramsey
Cavity

Optical
Pumping
Region

Cs Oven

Laser Diode
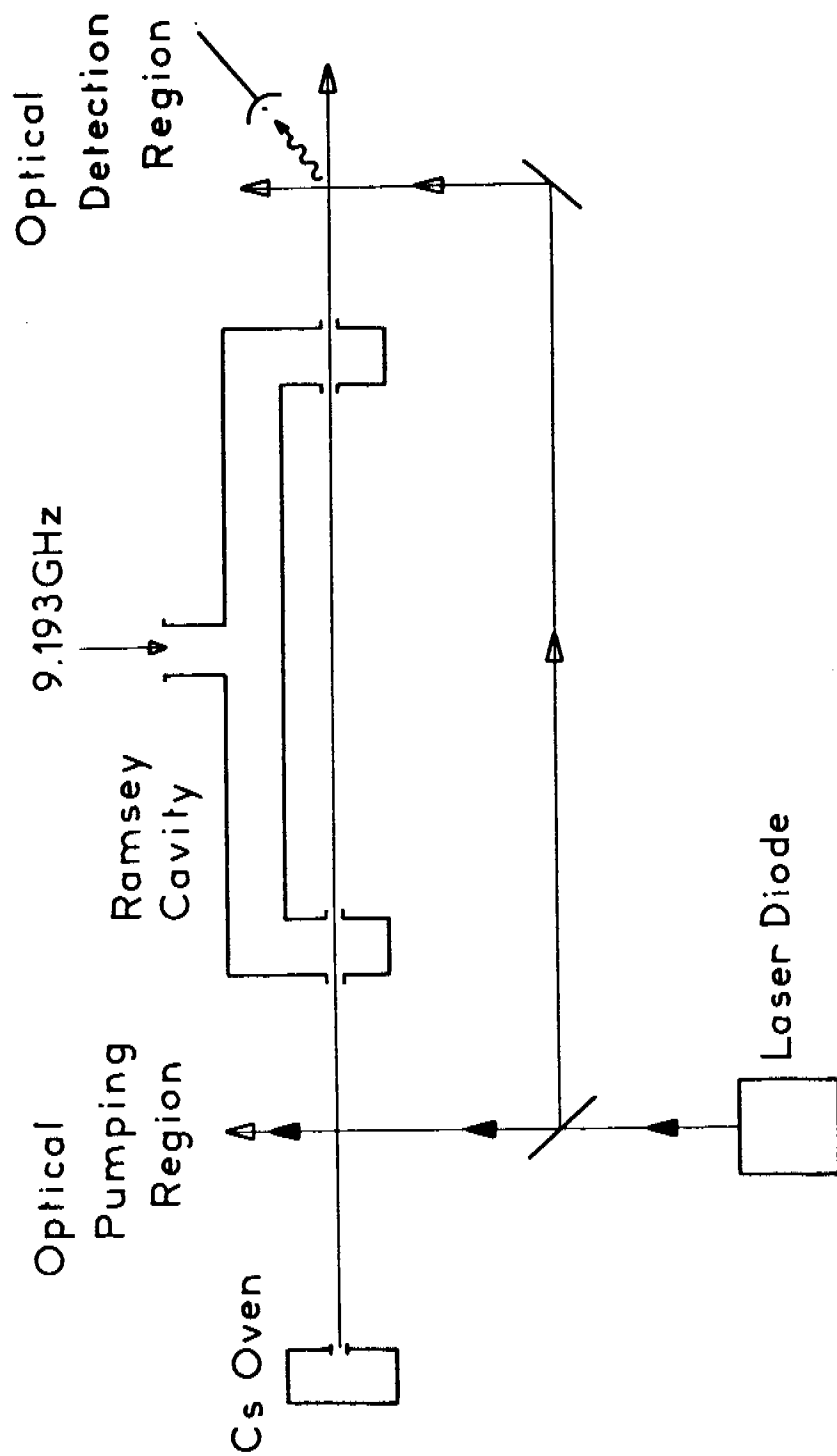
Cesium beam with one laser for optical pumping and detection.

Fig.3

30
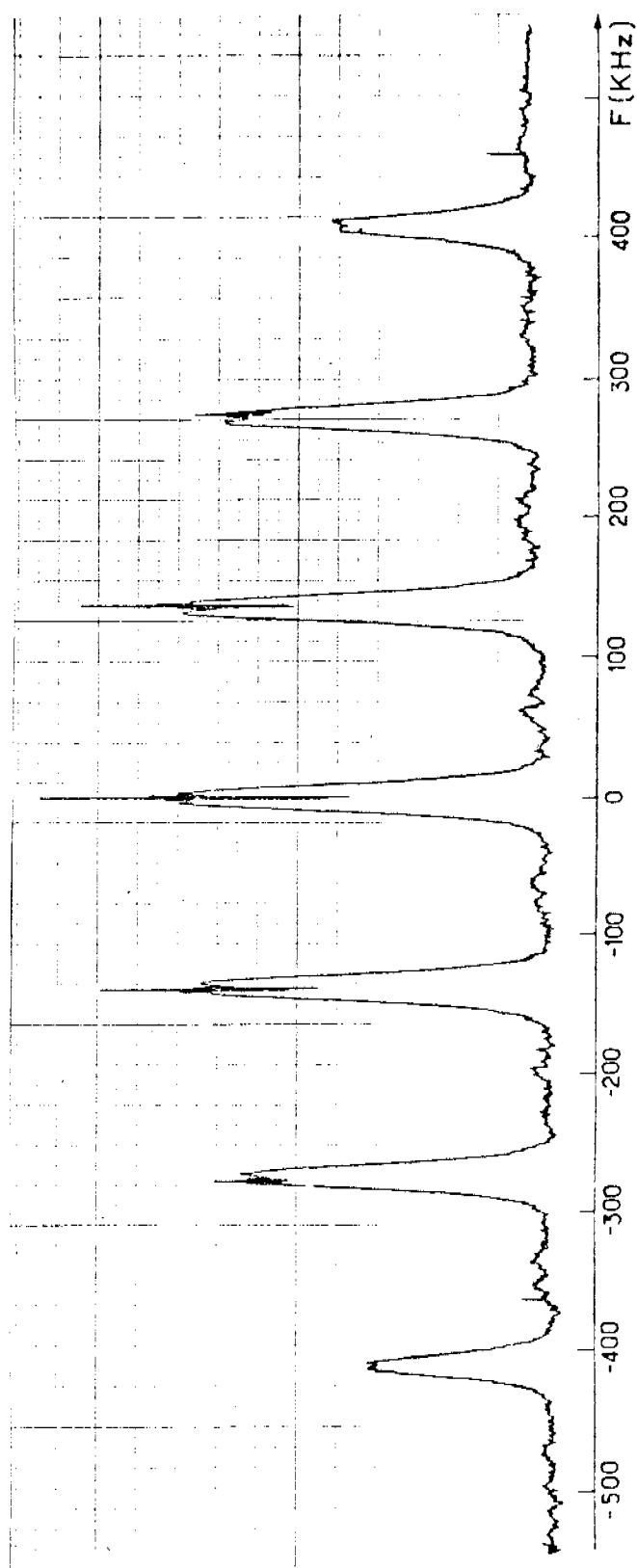
Microwave spectrum obtained with the one laser configuration.

Fig.4

31
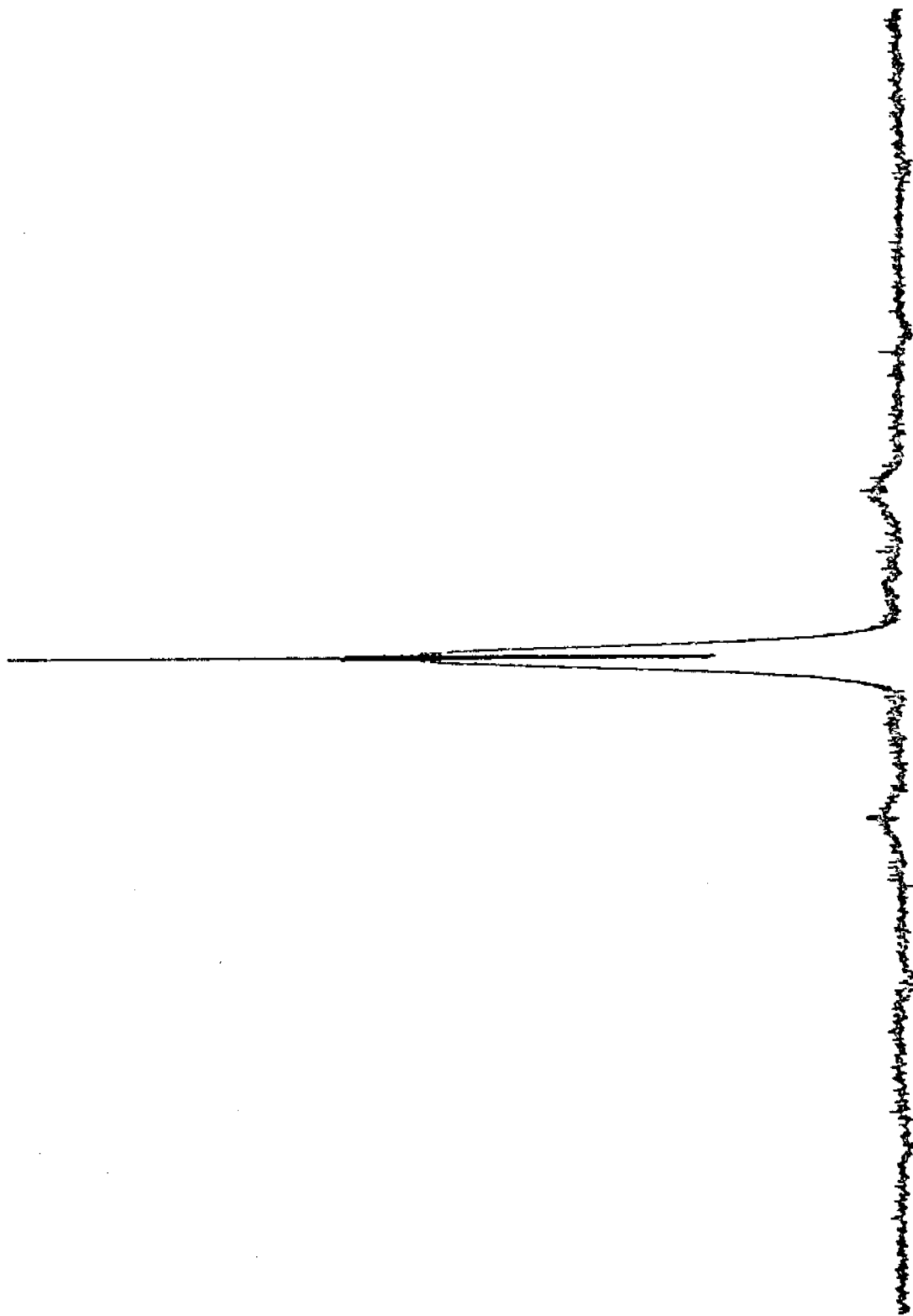
Microwave spectrum obtained with two lasers. Optical pumping : F = 3 ⟷
F' = 3 (π) and F = 4, F' = 3 (σ). Optical detection : F = 3, F' = 3 (σ). Same
horizontal scale as in Fig. 4.

Fig.5
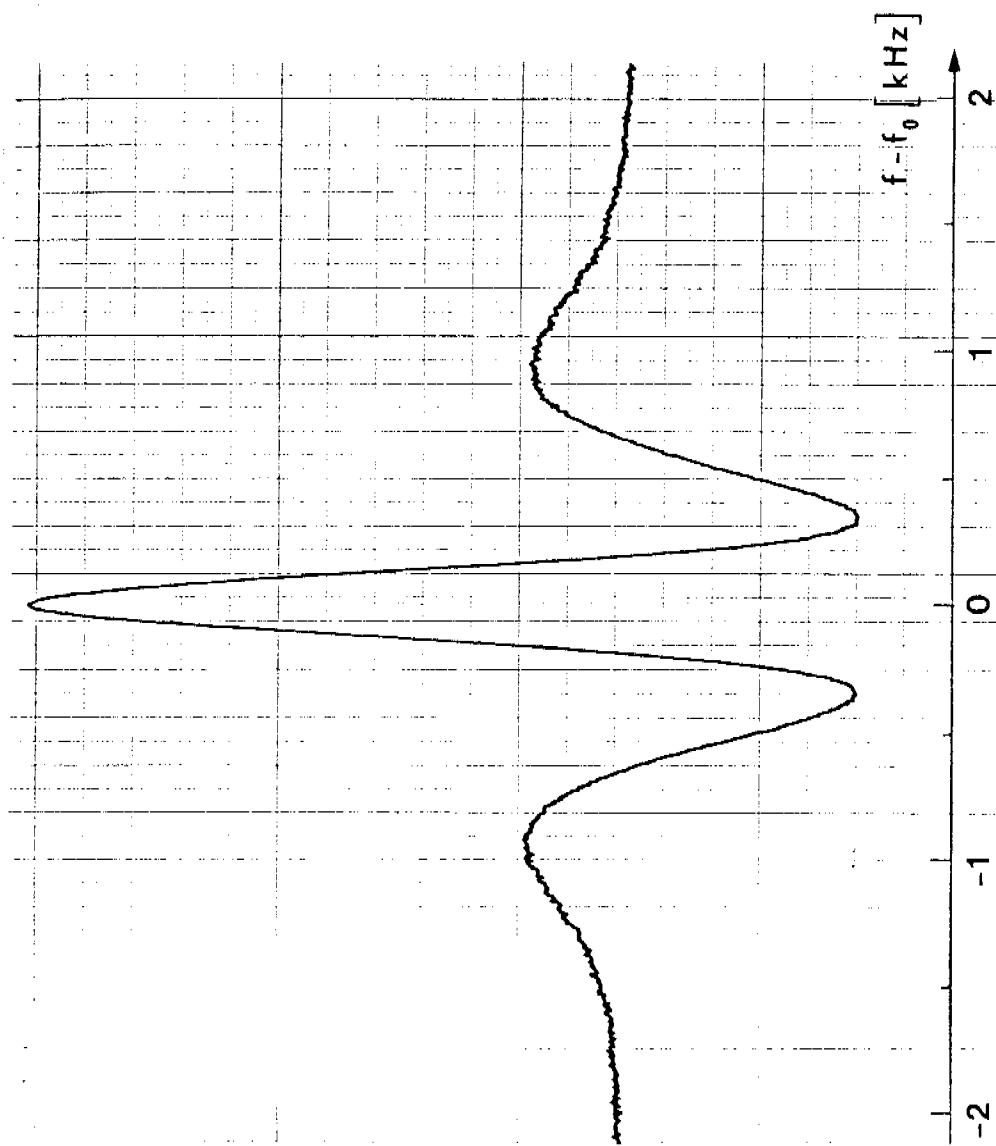
Central fringe of the Ramsey pattern obtained with two lasers for optical pumping and a third one for optical detection. We have : $\ell = 1$ cm, $L = 21,5$ cm and about optimum microwave power. The linewidth is 290 Hz.

Fig.6
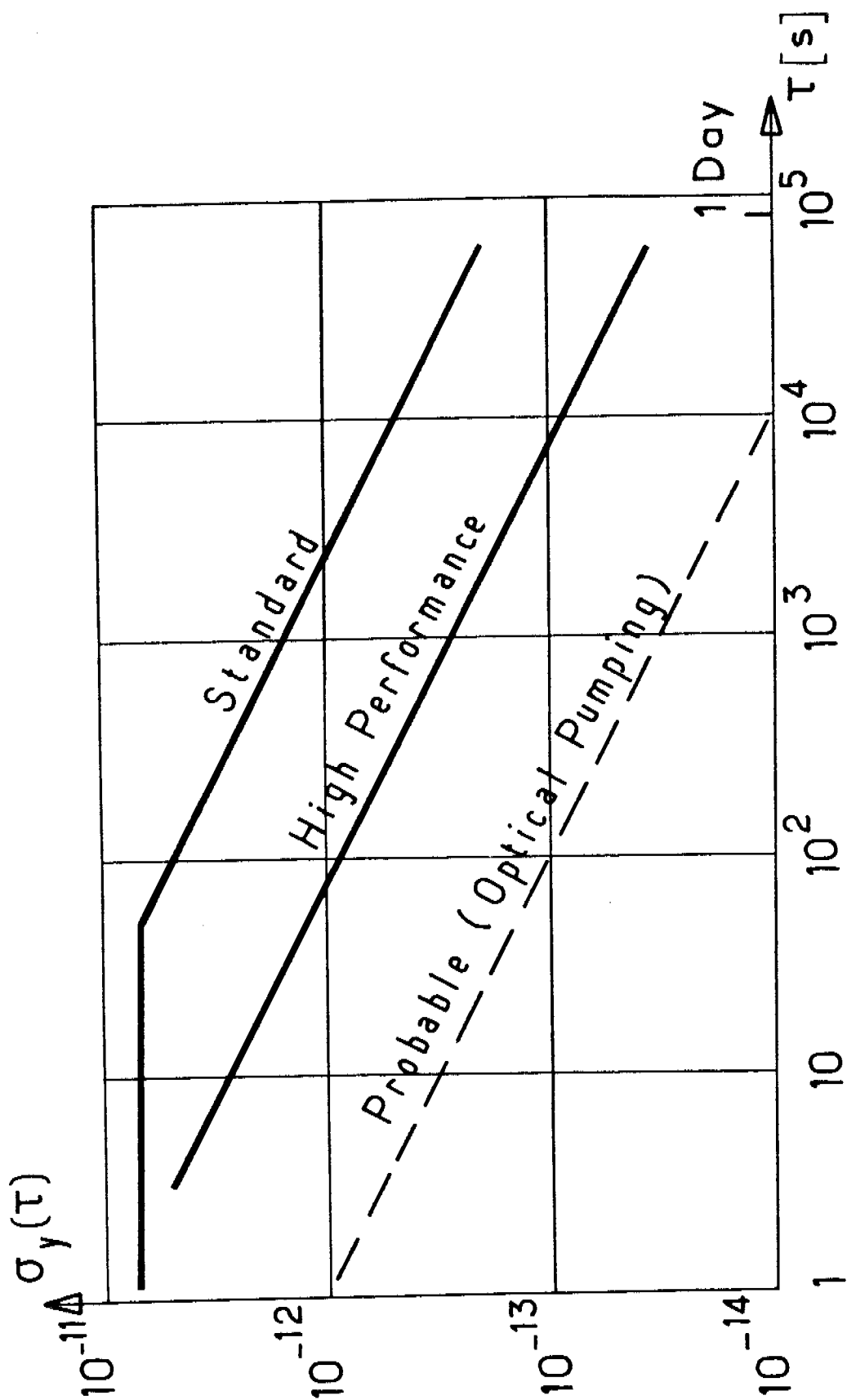
Example of frequency stability graph of two manufactured cesium beam frequency standards and expected frequency stability with optical pumping and detection methods. Standard:FTS 4050 model. High performance:HP 5061 A opt. 004 .

Fig.7
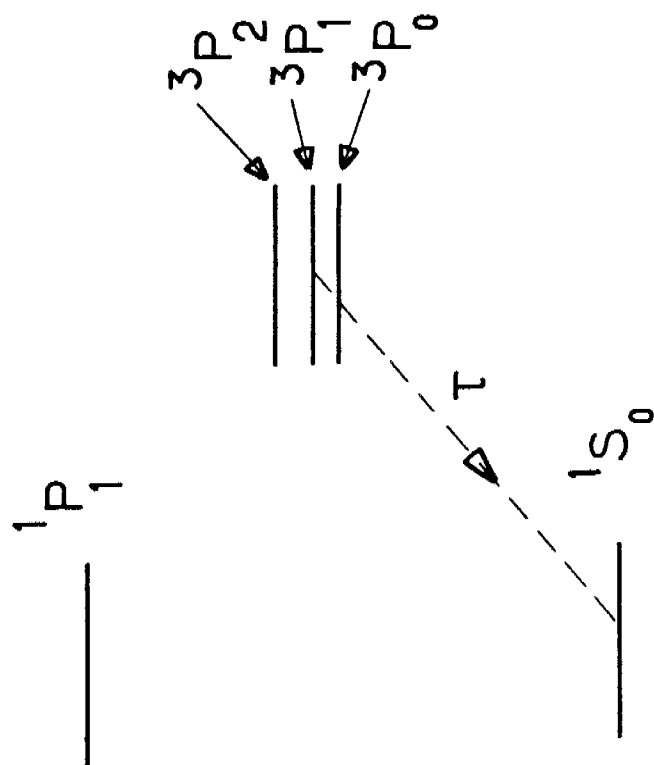
Simplified energy diagram of the first singlet and triplet levels of Mg and Ca. The life-time τ of the level $^3P_1$ is 4.6 ms for Mg and 0.55 ms for Ca.

Fig.8

Fig.9

Frequency stability graph of standard size VLG 11 hydrogen maser (from reference 30).
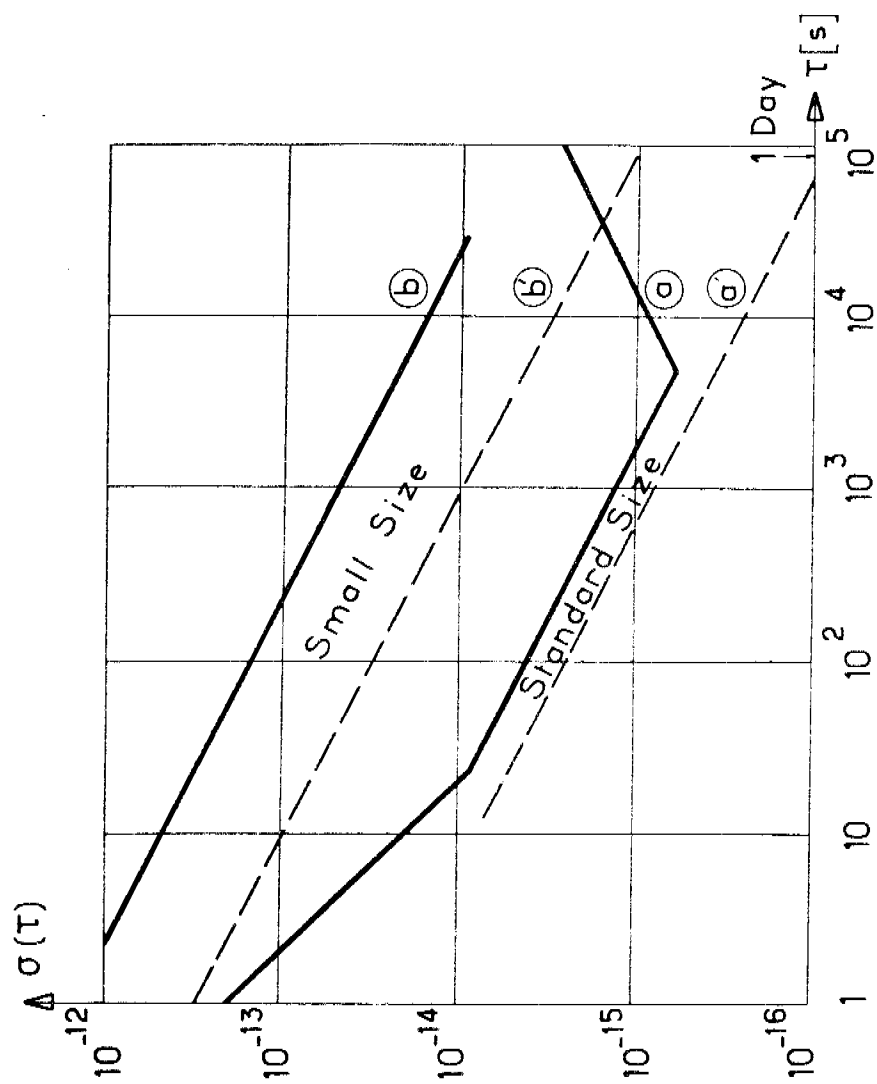
Frequency stability graph of hydrogen masers.

a. operational standard size hydrogen maser

a'. ultimate frequency stability of standard size hydrogen masers (room temperature)

b. operational small size hydrogen maser

b'. ultimate frequency stability of small size hydrogen masers (room temperature).

Fig. 10

Copper

Quartz

Dielectric
Material

b
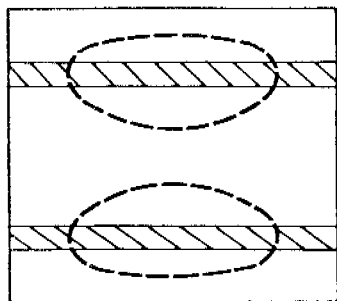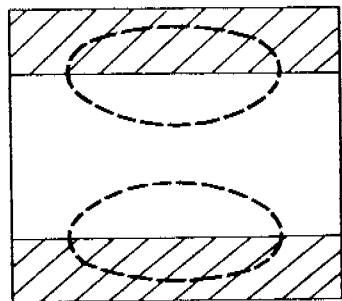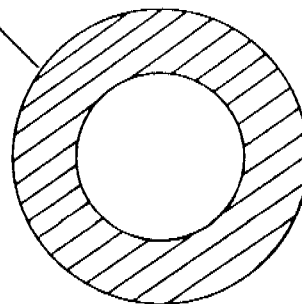
a

Resonant cavities for small size hydrogen masers

a. with a hollow cylinder of dielectric material

b. with conductors in the cavity.
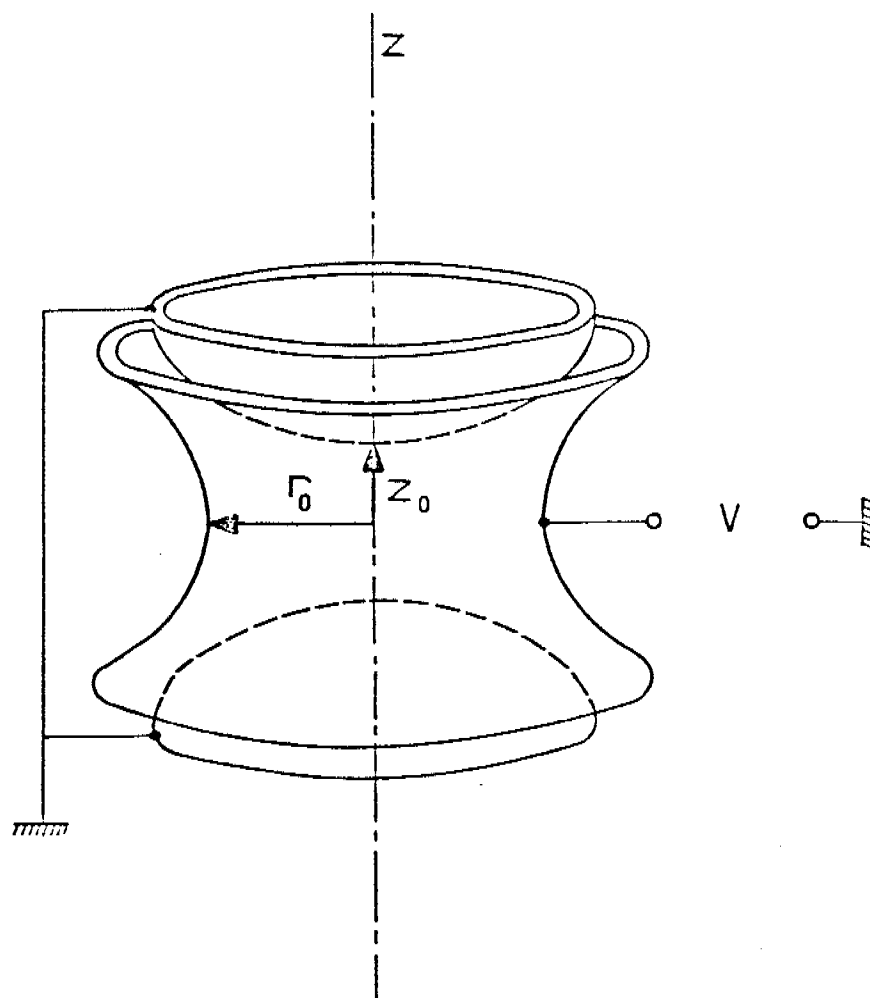
Dotted lines show the magnetic lines of force.
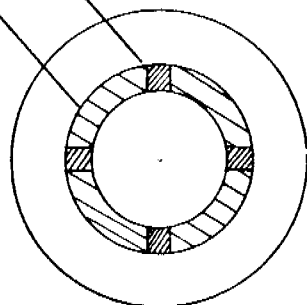
Fig.11

NBS SMALL PASSIVE HYDROGEN MASER PERFORMANCE
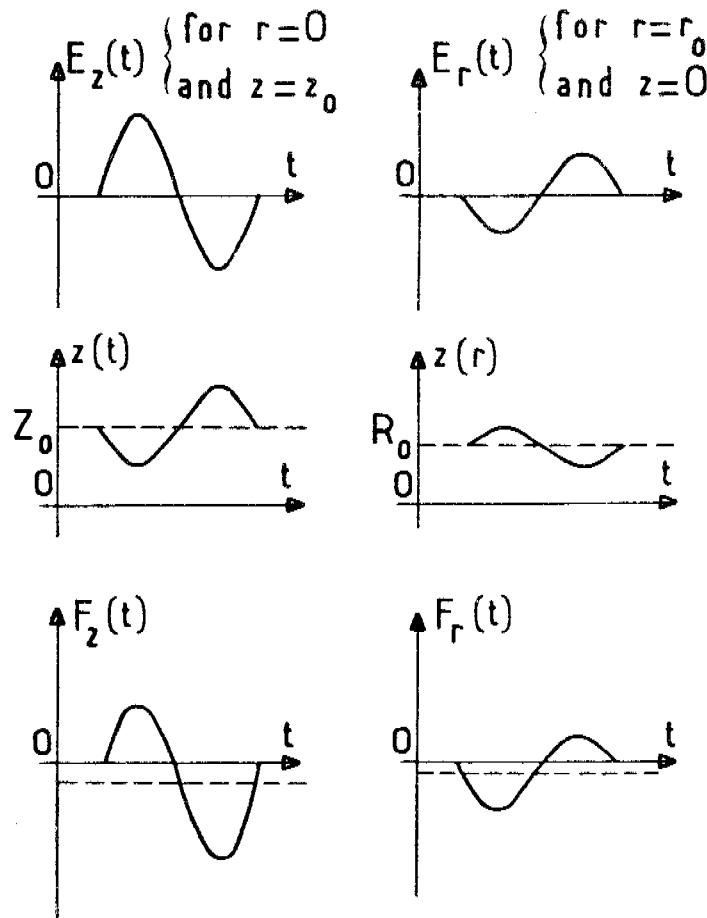
$1.7 \times 10^{-12} \tau^{-\frac{1}{2}}$
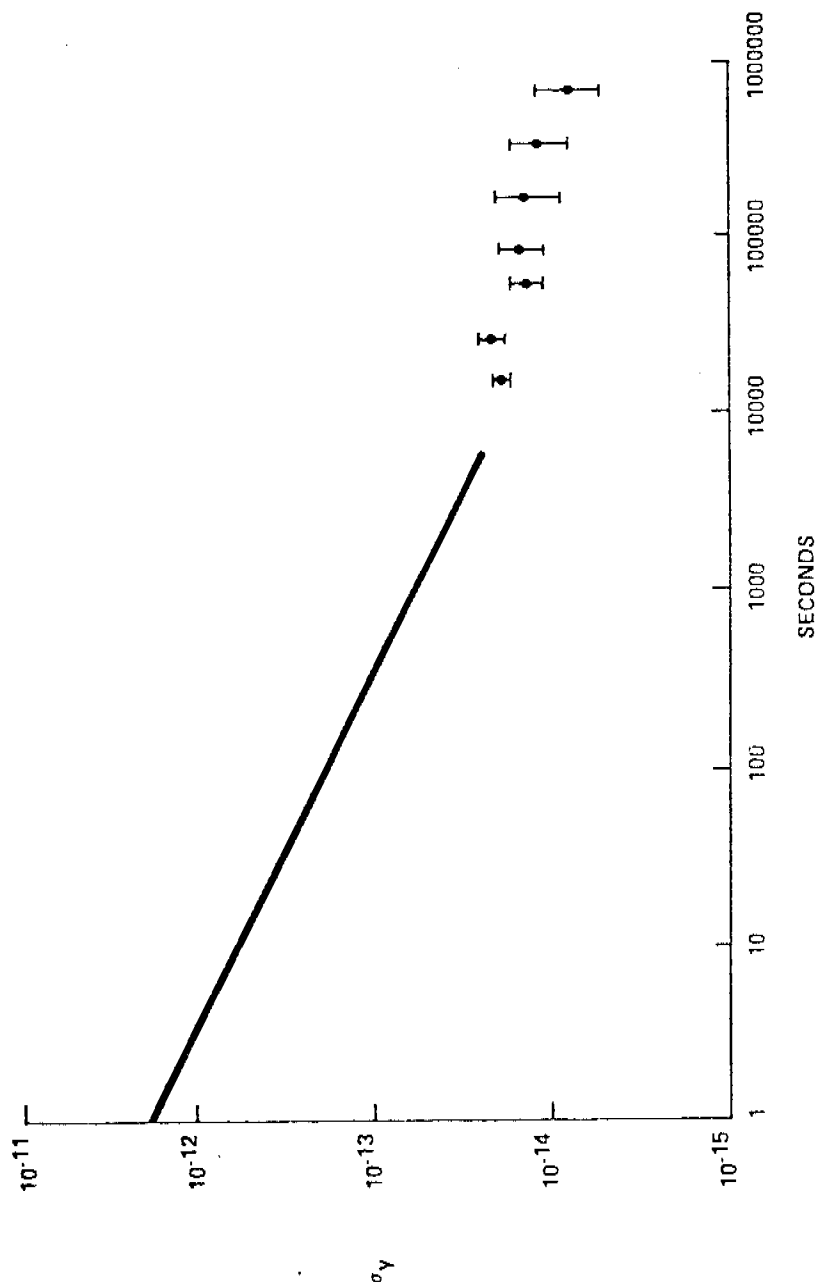
Frequency stability obtained with a passively operated small size hydrogen maser.

Fig.12

Electrodes of a ion trap, assuming a hyperboloïd shape.

Fig.13

$E_z(t)$ $\begin{cases} \text{for } r=0 \\ \text{and } z=z_0 \end{cases}$

$E_r(t)$ $\begin{cases} \text{for } r=r_0 \\ \text{and } z=0 \end{cases}$

$z(t)$

$z(r)$

$F_z(t)$

$F_r(t)$

Radiofrequency trap : origin of the axial (left) and transverse (right) confinement forces. The ionic charge is assumed positive.

Top : periodic variation of the axial electric field at point $r = 0$ and $z = z_0$ and of the transverse electric field at point $r = r_0$ and $z = 0$

Middle : Forced motion (micromotion) of the ion in the vicinity of the considered points

Bottom : Due to the electric field inhomogeneity, the variation of the axial and transverse components of the electric force is not sinusoïdal. It follows that the mean value of this force is not zero and it is directed towards the center of the trap. It yields the macromotion.

Fig.14
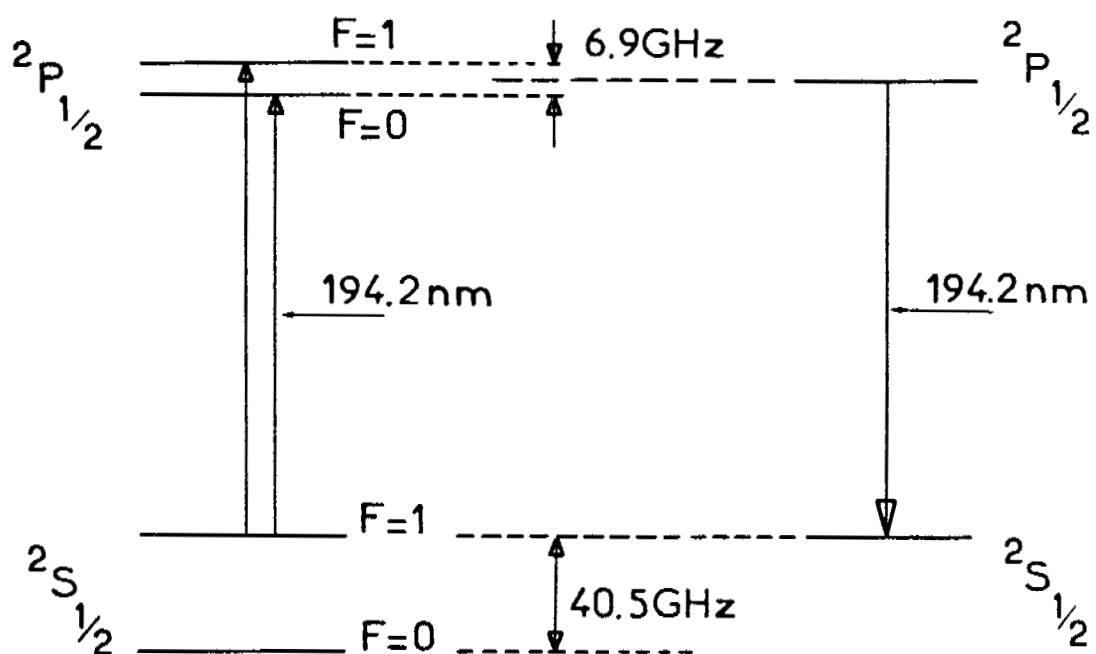
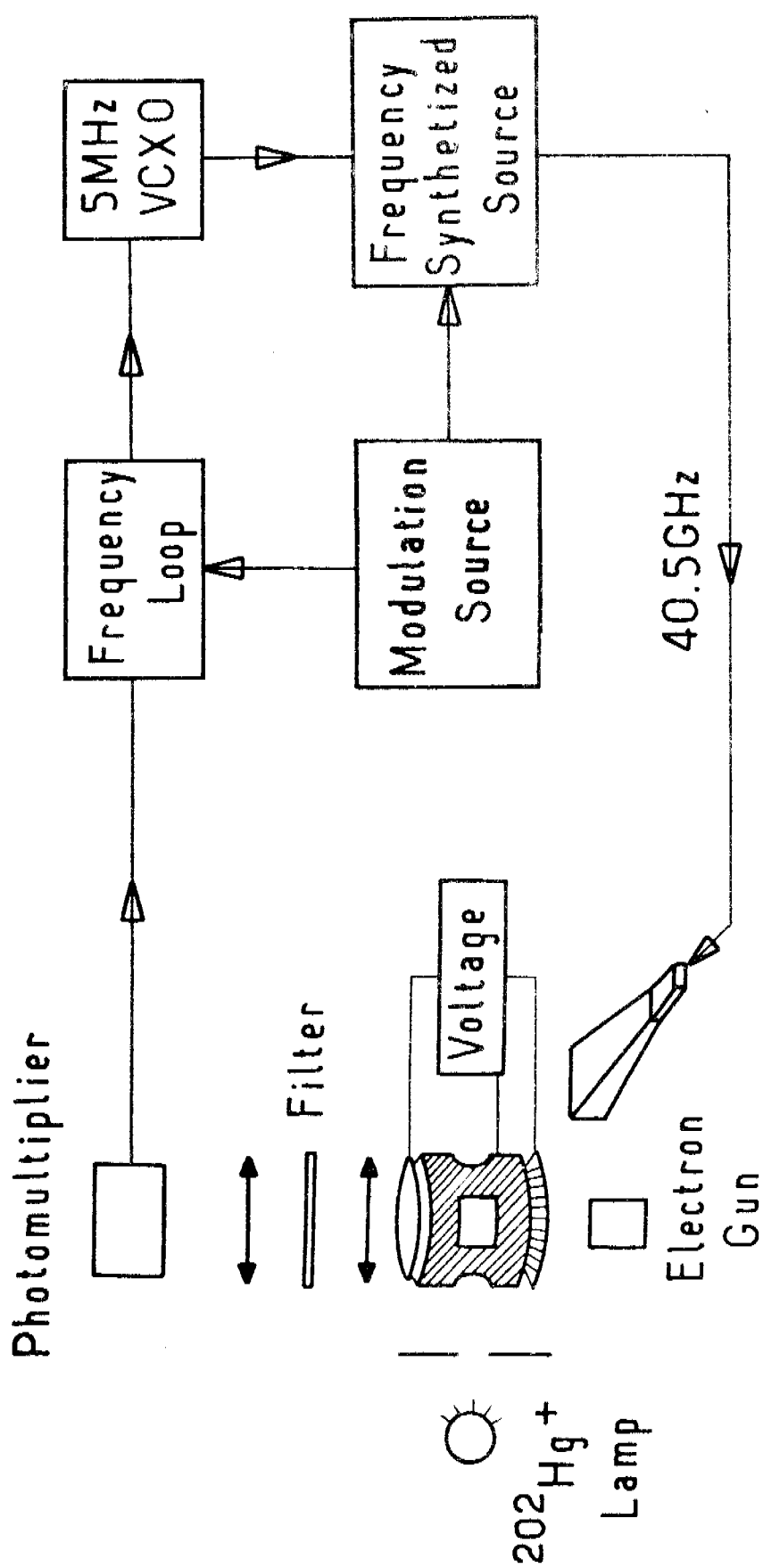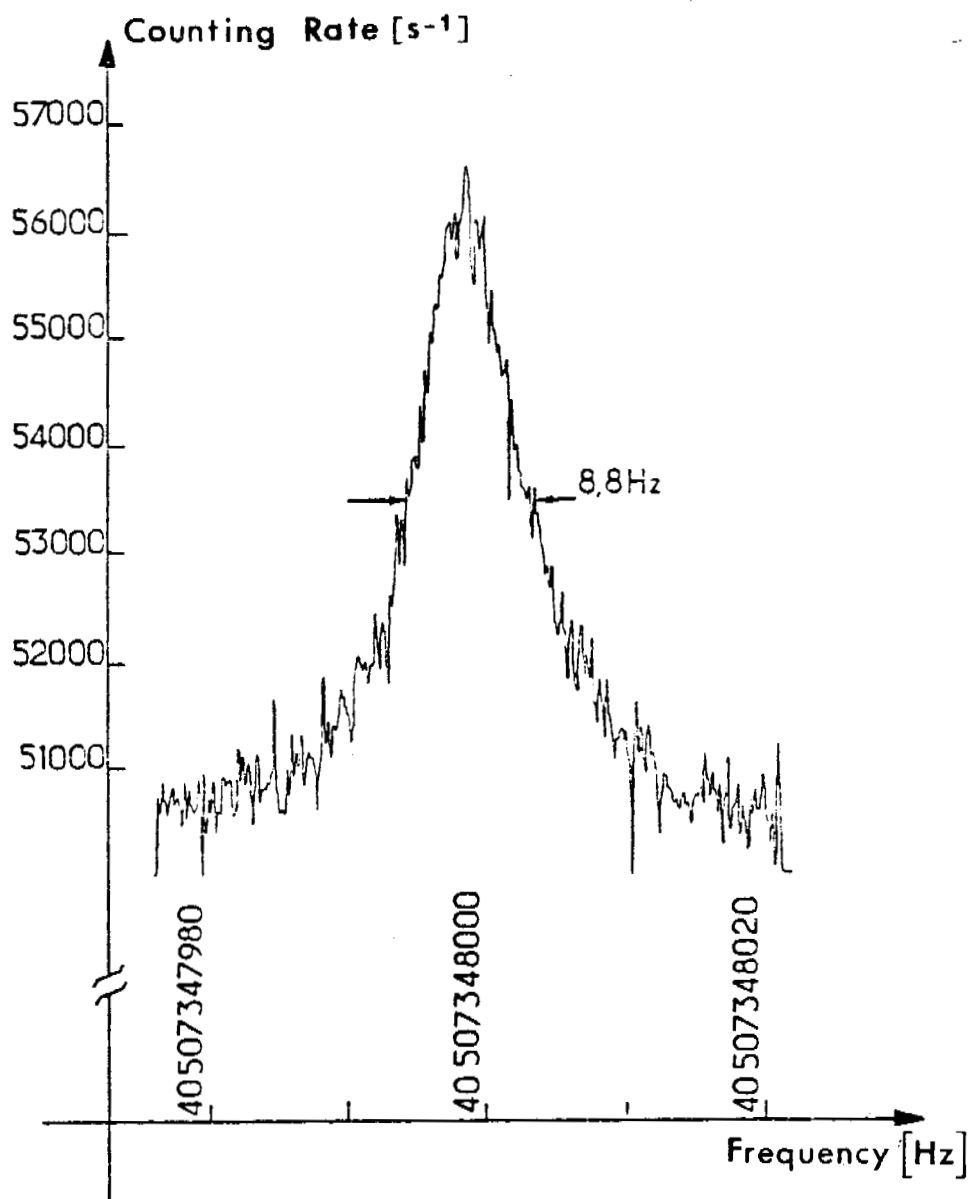Simplified energy diagram of $^{199}Hg^+$ and $^{202}Hg^+$.

Fig.15

Schematic representation of the mercury ion frequency standard set-up.

Fig.16

Photomultiplier

5MHz VCXO

Frequency Synthetized Source

Frequency Loop

Modulation Source

40.5GHz

Filter

Voltage

^{202}Hg$^+$ Lamp

Electron Gun

Power broadened hyperfine resonance line of $^{199}\text{Hg}^+$.

Fig.17
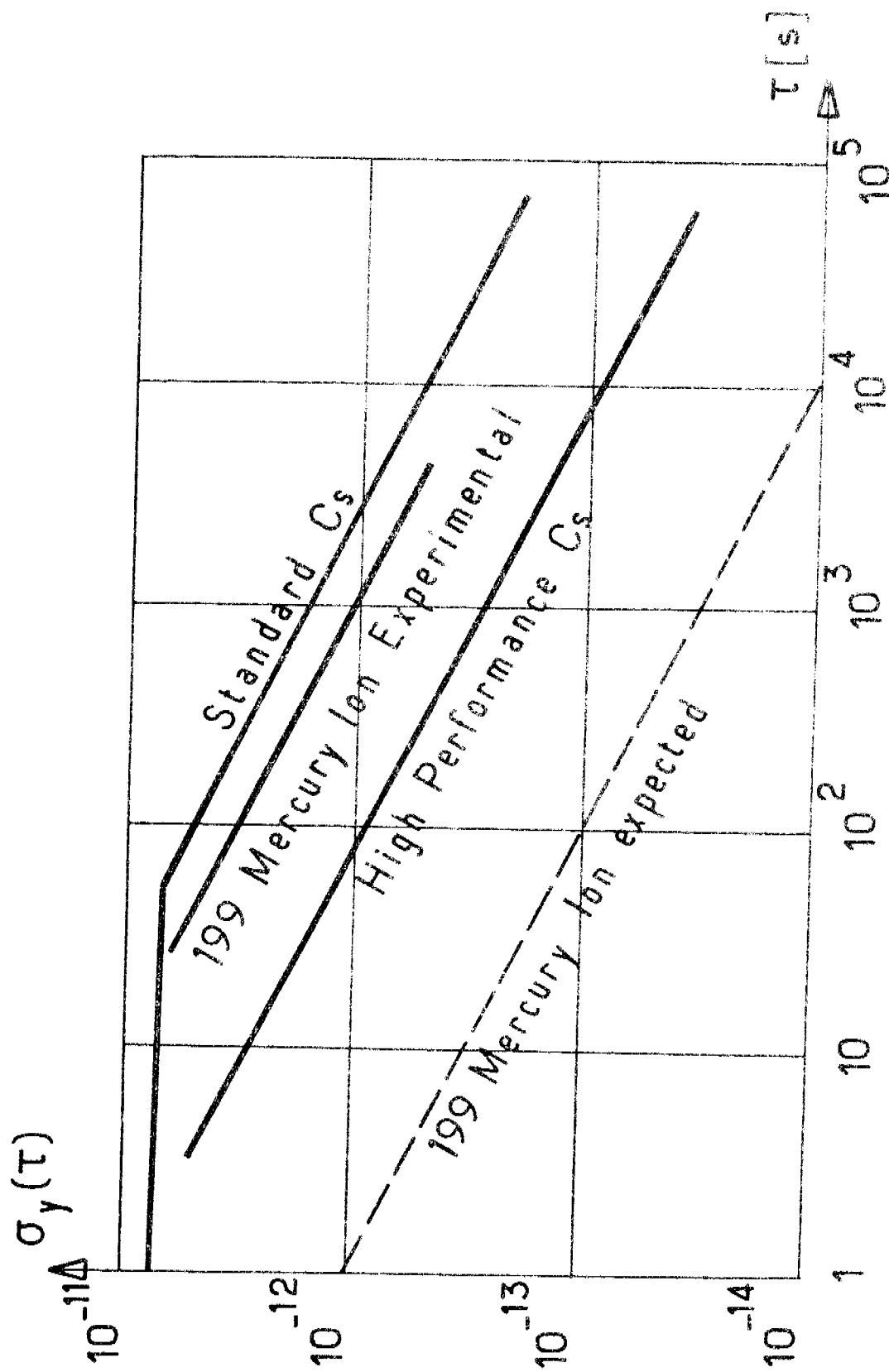
Frequency stability achieved in an experimental mercury ion frequency standard compared to portable cesium beam frequency standard. Dotted line: expected frequency stability.

Fig. 18

QUESTIONS AND ANSWERS

STUART CRAMPTON, WILLIAMS COLLEGE: I have saved most of my comments for tomorrow, but I would like to make two comments about cold hydrogen masers. One is that they are inherently small, and it's not necessary to use feedback in order to get oscillation. The second is the possibility of trade-offs. At a sacrifice of somewhat increased wall shift, one can operate at a lower temperature with the liquid helium walls and thus avoid the background pressure problem. So there are some interesting prospects in the future for that kind of device.

MR. AUDOIN: Yes, at the low temperature the linewidth is very small. The Q of the microwave cavity may be made extremely large using superconducting walls, or even copper has low losses at low temperature, so it is possible to have an active maser.

Also, it is possible to use, in principle, super conducting magnetic shields which reduce the problem of sensitivity to the magnetic field. So there are a lot of possibility of improvement.

VICTOR REINHARDT, HUGHES AIRCRAFT: Do you have any comments on the future possibility of a rubidium standard?

MR. AUDOIN: Yes, there is some indication in my manuscript on this, but I am not a specialist in rubidium clocks. Using optical pumping by diode lasers offers many new possibilities. As you know, in the present rubidium cells one uses a buffer gas for several purposes. One of them is to improve the optical pumping efficiency. But if you use a laser diode, the optical pumping efficiency will be large anyway, so we don't need the buffer gas. You may go to a wall coated cell, which will remove any difficulty due to that sense of motional variation in present rubidium cells. So, maybe one may expect improvements in that field, too.

MR. HELLWIG: Do you have any comment on the primary status of cesium versus the other techniques for the rest of the century?

MR. AUDOIN: Yes. The present level of performance of laboratory cesium standards is between one part in ten to the thirteenth and one part in ten to the fourteenth. I do not believe that it will be proved in this century that other devices have better accuracy. There are possibilities, ion storage gives the best promise in my view and there is a prospect with the cold hydrogen maser, but this has been proved with a different design of the device. I think that it will take time and I am confident that the definition will be attached to the cesium atom until the end of the century.

STEVE KNOWLES, NAVAL RESEARCH LABORATORY: While we are on the subject of frequency standards, I just wanted to mention the idea of frequency synchronization via phase length, via synchronous satellites. In a sense, this isn't a frequency standard at all, but if what one wants is worldwide frequency synchronization, this offers, I think, the possibility of accuracy on the order of

ten to the minus fifteenth, and since it's a true closed loop system, it has never been tested to see whether long term precision may be considerably lower than that.

MR. AUDOIN: Yes, but accuracy figure is attached to the device, not to the comprising system.

MR. KNOWLES: As I say, in a sense, I am not talking about the subject of your talk at all, but I wanted to say that if what one wants is worldwide frequency synchronization, then he can claim that this is equivalent to a secondary standard, and not a primary one.

MR. AUDOIN: Okay, these techniques allow comparison of standards.